

MODELING EPITHELIAL-MESENCHYMAL TRANSITION-INDUCED ERLOTINIB  
RESISTANCE IN NON-SMALL CELL LUNG CANCER

by  
Jessica Cades

A thesis submitted to Johns Hopkins University in conformity with the requirements for  
the degree of Doctor of Philosophy

Baltimore, Maryland

December, 2015

## Abstract

Lung cancer is the most common cause of cancer mortality throughout the world with an overall survival rate of around 17%. Adenocarcinoma is the most common histologic subtype of lung cancer, and a majority of human lung adenocarcinomas have somatic mutations in genes encoding members of the EGFR/KRAS/BRAF signaling pathway. Combining this knowledge with animal models of the pathway indicate that this signaling axis is of central importance to lung adenocarcinoma development. Non-small cell lung cancers with *EGFR* mutations, while initially responding well to EGFR tyrosine kinase inhibitors (TKIs) such as erlotinib, develop acquired resistance within 10-16 months. A relatively uncharacterized mechanism of resistance is lung cancer cells that have undergone a morphological change, termed epithelial-mesenchymal transition (EMT). Twist1 is one of the inducers of EMT and we have created a transgenic autochthonous lung cancer mouse model expressing *EGFR<sup>L858R</sup>/Twist1*. Using this novel *in vivo* model, as well as *in vitro* models, we have shown that overexpression of Twist1 can confer resistance to erlotinib in *EGFR* mutant lung cancers. Using these novel model systems we are trying to determine the downstream effects of Twist1 overexpression that lead to erlotinib resistance. To complement our work on Twist1-mediated erlotinib resistance, a bioinformatic-chemical screen was performed to identify potential pharmacological inhibitors of Twist1. From that screen, a promising class of agents, harmala alkaloids, was identified. Using human lung cancer cell lines to validate these agents has shown that several of the compounds have growth inhibitory effects. We tested one of the most promising compounds, harmine, *in vivo* with a transgenic *Kras<sup>G12D</sup>/Twist1* mouse model of autochthonous lung adenocarcinomas. When mice were

treated with harmine, tumor growth delay was observed by computed tomography imaging in harmine versus vehicle control mice. We are currently in the process of examining the molecular and cellular mechanisms of action of harmine using novel in vitro and in vivo model systems. These results are promising and provide a foundation for future experiments to determine if harmine, by inhibiting Twist1, can re-sensitize *EGFR* mutant lung cancers to erlotinib.

Thesis advisors:

Charles Rudin

Phuoc Tran

Thesis readers:

Timothy Burns

## Acknowledgements

*“Sometimes our light goes out but is blown into flame by another human being. Each of us owes deepest thanks to those who have rekindled this light.”*

– Albert Schweitzer

*“Everyone you will ever meet knows something you don’t.”*

– Bill Nye

Presented with the task of acknowledging all the people who have helped me reach this point is rather daunting. Mere words could never do justice the gratitude I feel for so many who have listened, consoled, encouraged, badgered, entertained, and supported me through the rollercoaster that this graduate program has been. I want to thank all those at Johns Hopkins who have played any role during my time at the institution. All my fellow classmates and lab mates, especially Linde Miles, Eric Gardner and Frank Vendetti, professors, administration, especially Amy Paronto, my thesis committee, Sam Denmeade and Mark Levis, the entire Pharmacology Department, and of course my PIs, Charlie Rudin and Phuoc Tran. I also want to thank all of my friends, both those I knew before moving to Baltimore and all the new friends I have made here; without all of you, graduating would not have been possible. The number of people who expressed how proud they are of my achievements is overwhelming and I consider myself extremely lucky to have such a great group of friends.

Lastly, I would like to thank my family. Despite not seeing each other on a regular basis, my entire family has always supported me in everything I do. My younger sister, Jenna, has always looked up to me and I have strived to be a good role model for



her. Finally, nothing I have ever achieved would be possible without the unwavering love and support from my parents. I only hope that I can continue to make you proud as the smallest token of my gratitude for all that you have done and continue to do for me.

## Table of Contents

Abstract .....	ii
Acknowledgements.....	iv
List of Tables .....	viii
List of Figures .....	ix
Chapter 1: Introduction.....	1
Chapter 2: Materials and Methods.....	14
Cell lines .....	14
Lentiviral overexpression experiments.....	14
Immunoblot analysis.....	14
Proliferation and viability assay.....	15
Transgenic mice .....	15
Histology and immunohistochemistry.....	16
PathScan RTK antibody array kit.....	17
Microarray data acquisition and analysis.....	17
Chapter 3: Characterization of TWIST1 mediated acquired resistance to Erlotinib in EGFR mutant lung cancer cell lines.....	19
Section 3.1: Results.....	19
Section 3.2: Discussion.....	23
Section 3.3: Conclusions.....	24
Chapter 4: Creation and Characterization of an Autochthonous <i>EGFR</i> Mutant Lung Tumor Model .....	25
Section 4.1: Results.....	25
Section 4.2: Discussion and Conclusions .....	29
Chapter 5: Investigation of the Mechanisms of Twist1-induced Erlotinib Resistance in a mouse model of EGFR Mutant Lung Cancer .....	31
Section 5.1: Results.....	31
<i>Twist1</i> expression results in erlotinib resistance.....	31
Characterization of Twist1 induced resistance.....	35
Validation and investigation of Src target.....	38
Combination treatment with erlotinib and dasatinib overcomes resistance resulting from <i>Twist1</i> expression.....	42
Bioinformatic Analysis of Erlotinib Resistance .....	44
Section 5.2: Discussion.....	49
Section 5.3: Conclusions.....	51

Chapter 6: Identification and Characterization of a novel TWIST1 inhibitor .....	52
Section 6.1: Introduction.....	52
Section 6.2: Materials and Methods.....	58
Immunoblot analysis .....	58
Histology and immunohistochemistry .....	58
Transgenic mice .....	59
Section 6.3: Results.....	60
Section 6.4: Discussion and Conclusions .....	64
Chapter 7: References .....	66
Curriculum vitae .....	75

## List of Tables

Table 5.1. Top significant gene sets.....	46
Table 5.2. Top significant genes.....	47

## List of Figures

Figure 1.1. EGFR Tyrosine Kinase Inhibitor (TKI) mechanisms of acquired resistance...	4
Figure 1.2. Altered EGFR signaling in NSCLC. ....	6
Figure 1.3. EMT is a dynamic process. ....	9
Figure 1.4. Cross-cancer alteration summary for TWIST1 from cBio portal.....	11
Figure 3.1. Overexpression of TWIST1 alters levels of phosphorylation downstream of EGFR in vitro.....	21
Figure 3.2. Overexpression of TWIST1 confers erlotinib resistance in a subset of <i>EGFR</i> mutant cell lines. ....	22
Figure 4.1. Generation and characterization of a novel Twist1 overexpressing, mutant EGFR autochthonous lung tumor mouse model.....	27
Figure 4.2. Generation and characterization of a novel Twist1 overexpressing, mutant EGFR autochthonous lung tumor mouse model.....	28
Figure 5.1 Twist1 expression results in erlotinib resistance.....	32
Figure 5.2. Twist1 expression alters tumor burden and response to erlotinib treatment. .	34
Figure 5.3. Characterization of Twist1 induced erlotinib resistance. ....	36
Figure 5.4. Twist1 expression alters phosphorylation levels of RTKs and signaling nodes. ....	37
Figure 5.5. Validation and Investigation of Src target.....	40
Figure 5.6. Combination treatment decreases downstream phosphorylation.. ....	41
Figure 5.7. Combination treatment with erlotinib and dasatinib overcomes resistance resulting from Twist1 expression.....	43
Figure 5.8. Ingenuity Pathway Analysis. ....	48
Figure 6.1. Overview of CMap Analysis.....	56
Figure 6.2. . Harmine inhibits growth through degradation of TWIST1 in oncogene driver define NSCLC cell lines. ....	57
Figure 6.3. Harmine has activity in a KrasG12D/Twist1 murine model of lung adenocarcinoma. ....	61

Figure 6.4. Harmine treatment alters some cellular processes in a *Kras*G12D/*Twist1* murine model of lung adenocarcinoma..... 62

Figure 6.5. Harmine decreases *Twist1* levels in a *Kras*<sup>G12D</sup>/*Twist1* murine model of lung adenocarcinoma. .... 63

## Chapter 1: Introduction

Lung cancer is the leading cause of cancer mortality in the United States, resulting in more deaths than prostate, breast, and colorectal cancers combined. Most lung cancers are diagnosed at an advanced stage and tend to be treatment resistant, leading to an estimated overall survival rate of a mere 17% (1). Non-small cell lung cancer (NSCLC) accounts for more than 80% of lung cancers and includes two major types, non-squamous carcinoma, which includes adenocarcinoma, the most common type of lung cancer in the United, and squamous cell carcinoma. Patients with locally advanced (stage III) and metastatic (stage IV) NSCLC comprise more than 50% of patients with lung cancer. Several biomarkers serve as prognostic or predictive makers in NSCLC, including the presence of *ALK* alterations, *KRAS* and *epidermal growth factor receptor (EGFR)* mutations. Surgery, radiation therapy and chemotherapy are the three methods most common for treatment of patients with NSCLC. Depending on the disease stage, they can be used alone or in combination (2).

A growing and increasingly important class of drugs for cancer treatment is targeted therapies, specifically tyrosine kinase inhibitors (TKIs). This is due to advancements in knowledge of genetic and molecular features of patient's cancer, such as mutational status of specific oncogenic drivers (3). In NSCLC, especially, targeted therapies have improved outcomes for patients with a variety of molecular profiles, leading to complete and durable responses (4). The success of these therapies is due to the oncogene addicted nature of some tumors. In these tumors, mutations lead to constitutive activation of receptor tyrosine kinases (RTKs), which then are able to

activate downstream signaling pathways, enabling cancer growth. Inhibiting the RTK, with a targeted therapy, results in suppression of all the activated downstream pathways, leading to cell growth arrest and death and ultimately tumor regression (5, 6).

Targeted therapies, such as TKIs, are a preferential method of treatment, as they have high specificity for tumor cells resulting in less toxicity to healthy cells and a broader therapeutic window (7). The first generation of EGFR TKIs, which includes erlotinib, is orally available, quinazoline-based small molecules. These molecules reversibly inhibit the ligand-induced phosphorylation by competing with adenosine-triphosphate (ATP) for binding with the intracellular catalytic domain of EGFR (8). While EGFR TKIs have activity against wild type EGFR, the activating mutations in EGFR, the exon 19 deletion and L858R mutation, confer increased sensitivity to the targeted agents. These mutations cluster near the ATP binding pocket of EGFR. Since erlotinib competes with ATP at this site, the mutations have been hypothesized to increase the affinity for the small molecule over ATP or to stabilize the interaction between EGFR and erlotinib (9-11).

While targeted therapies have advanced treatment, acquired resistance is seemingly inevitable. Some cancers are intrinsically resistant to therapy and acquired resistance commonly develops after 1-2 years, regardless of whether the treatment was first-line or subsequent. Formal criteria to define acquired resistance exist for some types of oncogene driven tumors, but in general it is any evidence of clinical progression after initial clinical benefit. In lung cancer patients that have oncogene-addicted cancers, there are two main types of acquired resistance, pharmacological and biological.

Pharmacological resistance is due to inadequate on-target drug exposure. More common



is biologic resistance in which resistant cancer subclones emerge under the selective pressure of a targeted inhibitor (4). Targeted therapy resistance is a common occurrence, not just in lung cancer treatment, and understanding basic mechanisms of the biologic resistance could potentially allow for prevention of resistance, leading to sustained responses, as well as facilitating design of therapies that will be more effective in the long term. Four common general mechanisms of targeted therapy resistance include target reactivation, activation of “downstream” effectors, bypass of the (onco) protein effector and adaptation (3, 12). As illustrated in Figure 1.1, acquired resistance to an EGFR TKIs, actually takes advantage of each of these mechanisms.

Target reactivation can occur through a secondary mutation in the kinase target, changing the affinity for the TKI or the affinity for an effector molecule. Activation of downstream effectors can result from mutations in or modification of expression levels of molecules that are downstream of the initial kinase target in the signaling pathway. The complete bypass of the kinase can occur through modification of the expression of another tyrosine kinase that activates the same or complimentary signaling pathway (3).

One of the most targetable mutated driver oncogenes in NSCLC, as previously mentioned, is *EGFR*, with around 20% of adenocarcinomas possessing an *EGFR* mutation. The highest prevalence is seen in female never-smokers. The two most common mutations are an exon 19 deletion or an exon 21 L858R point mutation. The mutations are mutually exclusive and their presence is strongly predictive of benefit (ORR 60-70%) from an EGFR TKI, such as erlotinib (11, 13). This molecular phenotype distinguishes *EGFR* mutant disease as a distinct category of NSCLC.

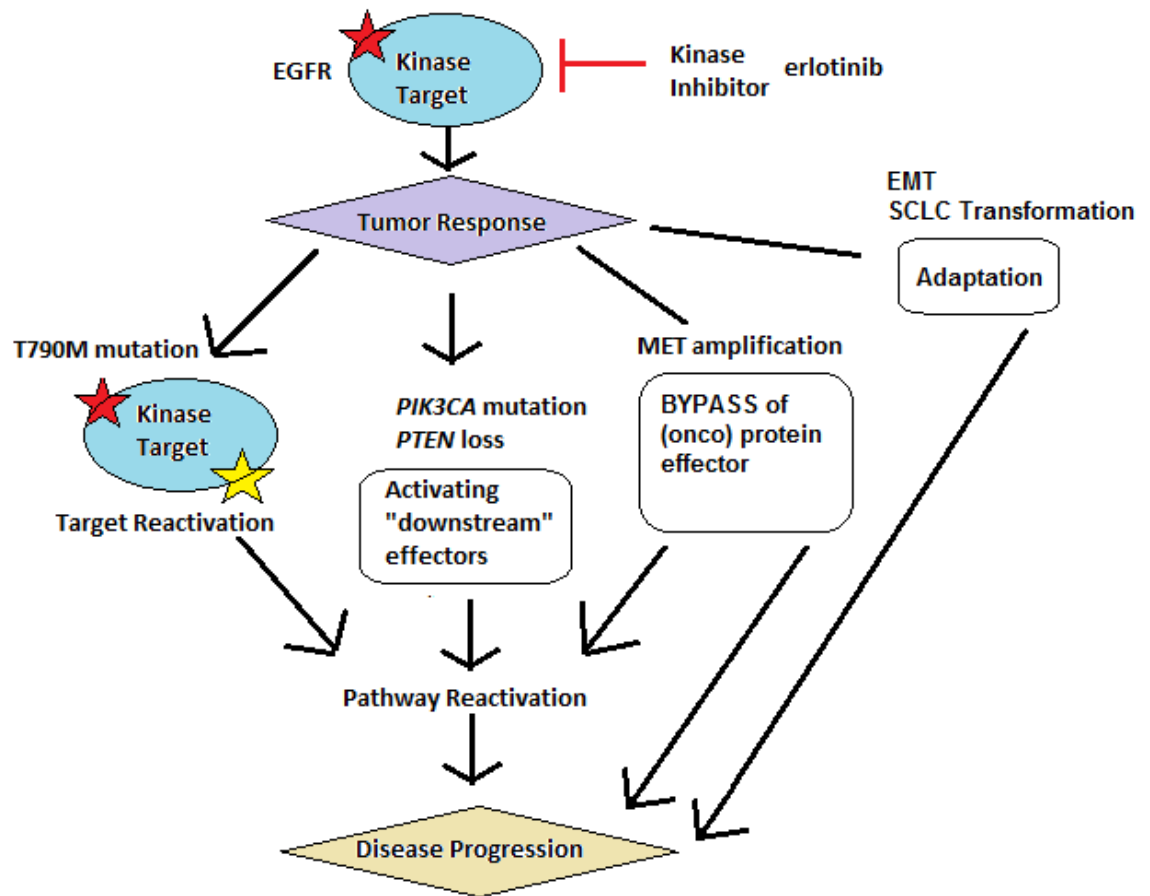


**Figure 1.1. EGFR Tyrosine Kinase Inhibitor (TKI) mechanisms of acquired resistance.** Adopted from Garraway and Jänne, *Cancer Discovery* 2012; 2:214-226. Erlotinib is an EGFR TKI and patients with exon 19 deletions or L858R mutations in *EGFR* frequently have initial great responses to the drug. However, acquired resistance occurs, through several known and unknown mechanisms. The known mechanisms include a secondary mutation in *EGFR*, *EGFR*<sup>T790M</sup>, *PTEN* loss or *PIK3CA* mutation, and *MET* amplification. Patients commonly see the return of their disease within a year of erlotinib therapy.

EGFR is a member of the ErbB RTK family and is activated by secreted growth factors, which leads to dimer formation, increase in kinase activity, phosphorylation of intracellular tyrosine residues, and activation of signaling pathways as can be seen in Figure 1.2. In cancer, overexpression of EGFR conveys several advantages that promote cell proliferation, survival, angiogenesis, invasion and metastasis. Mutations in EGFR lead to increased activity and ligand independent dimerization and phosphorylation. As a result of this amplified EGFR signaling activity, the PI3K/Akt and STAT signaling pathways appear to be most affected. This promotes the increased cell proliferation and survival, partially through inhibition of apoptosis, as well as tumorigenesis (14).

Despite the initial dramatic response to erlotinib, after an average duration of response of approximately 12 months, disease progression occurs due to acquired resistance to erlotinib and other EGFR inhibitors (12). Primary resistance tends to be less common and thus it is the mechanisms of acquired or secondary resistance that have warranted more investigation. The most common mechanism of acquired resistance to EGFR TKIs, accounting for >50%, is the presence of a second site *EGFR* mutation, T790M. This residue is located in the hydrophobic ATP-binding pocket of the catalytic region, and the mutation prevents the formation of a hydrogen bond essential for the TKIs' action (15). A second mechanism of acquired resistance is amplification of the gene encoding the MET receptor tyrosine kinase. About 15-20% of cancers demonstrate this amplification, which is not mutually exclusive with the T790M mutation. *MET* amplification activates downstream intracellular signaling independent of EGFR via ERBB3 (16, 17). Other less common mechanisms of resistance include mutations in *PIK3CA* (~5%) and *PTEN* loss, both impacting the Akt signaling pathway, amplification

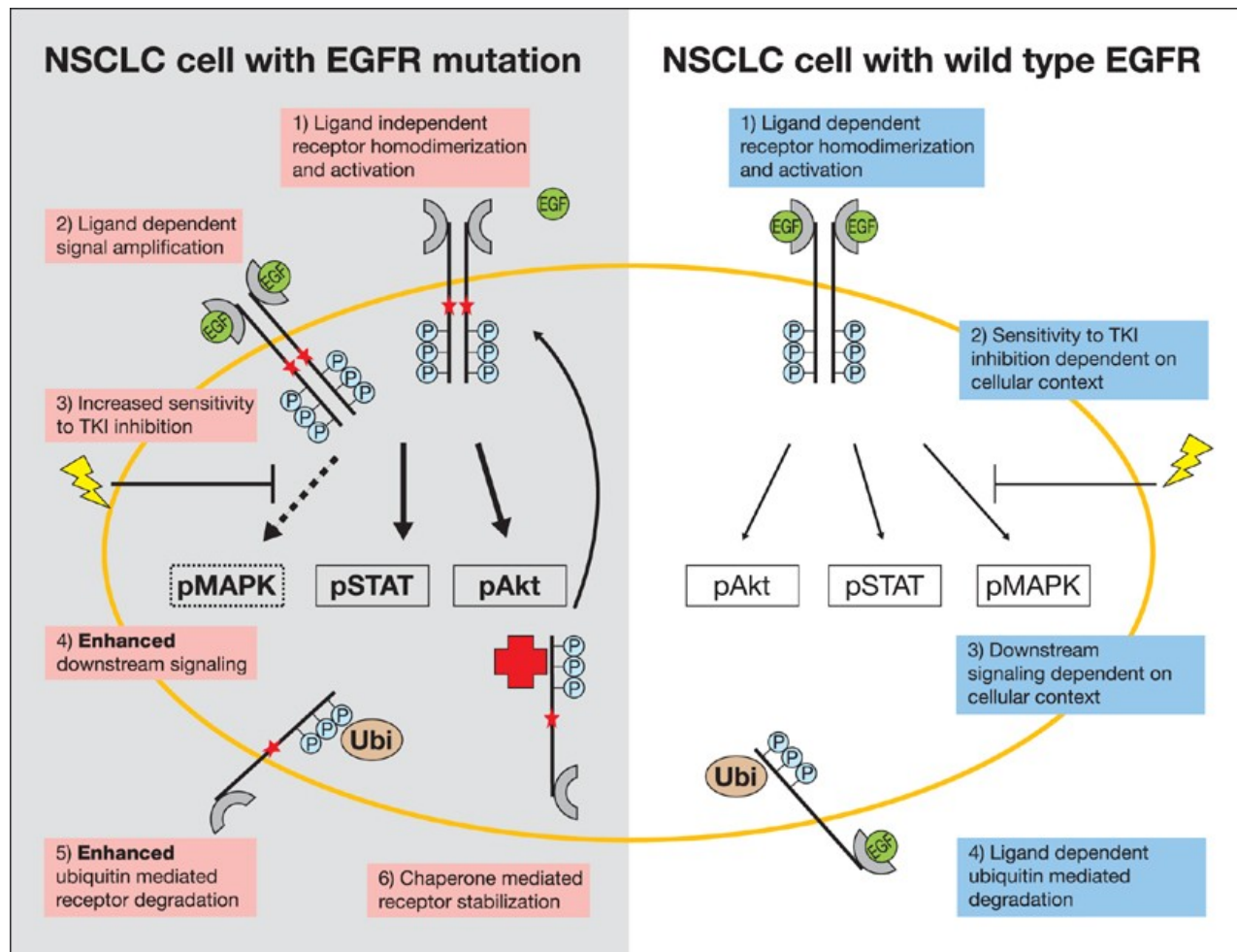


**Figure 1.2. Altered EGFR signaling in NSCLC.** From Imer D, Funk JO, Blaukat A. EGFR kinase domain mutations - functional impact and relevance for lung cancer therapy. *Oncogene*, 2007. Comparison of EGFR signaling in wild type versus mutant EGFR NSCLC.

of *HER2*, as well as transformation from NSCLC to small cell lung cancer (SCLC) and epithelial-mesenchymal transition (EMT) (12, 18, 19).

Despite the large effort to understand the mechanisms of acquired resistance to erlotinib, and targeted therapies in general, a significant portion of acquired resistance cases have an unknown mechanism (12). A potential and less well defined mechanism, accounting for anywhere from 5-30% of cases, is that of epithelial lung cancer cells that have undergone a morphological change to a more mesenchymal phenotype, better known as having undergone EMT (12, 20). Many groups have utilized cell lines and patient samples to show a correlation between EMT and EGFR TKI acquired resistance, however direct causation and the mechanism of how EMT is preventing the drugs from being effective has yet to be established (12, 21-29).

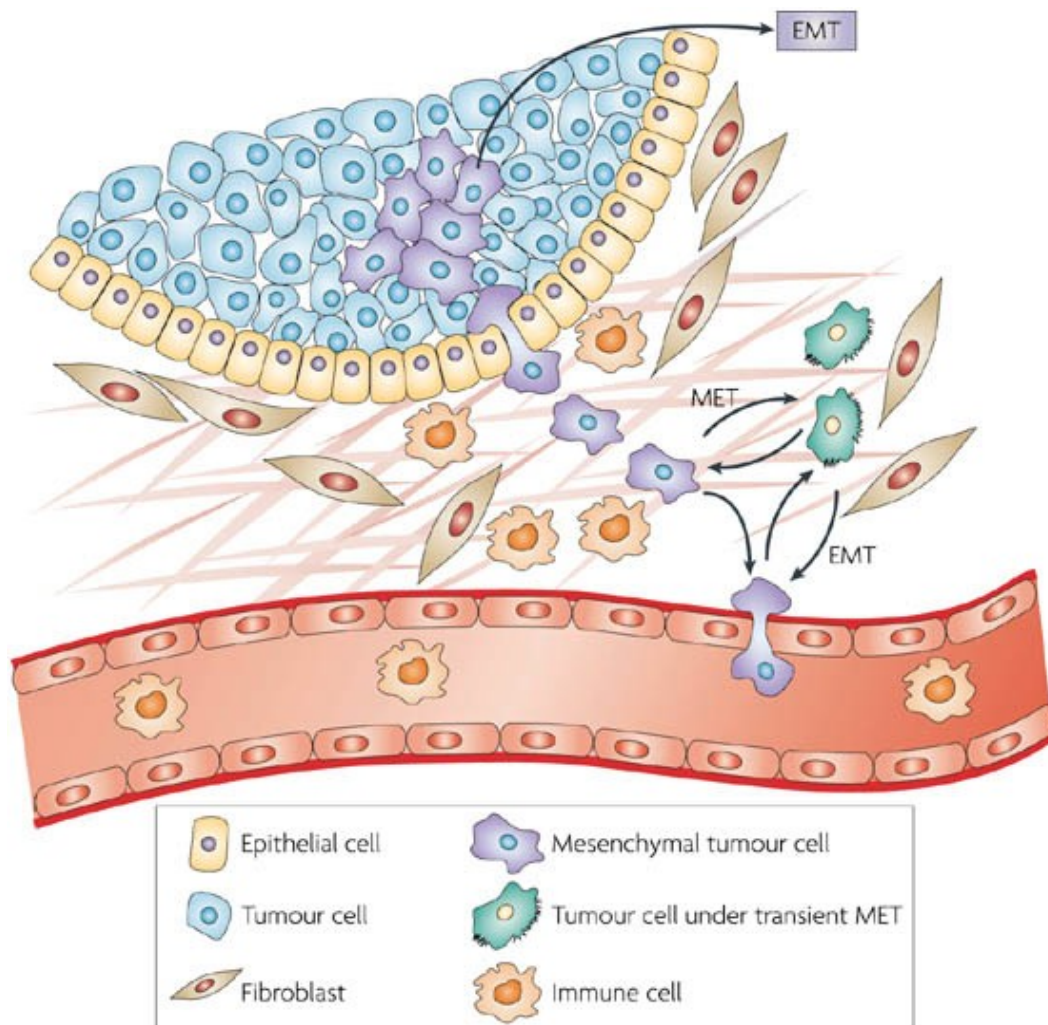
EMT is a highly conserved cellular program that allows for epithelial cells to convert to mesenchymal cells, resulting in a loss of polarity and an increase in motility. The process was identified nearly 40 years ago and subsequently defined as a distinct cellular program in the 1970-80s and has been loosely defined by three major changes in cellular phenotype (30-33):

- (1) morphological changes from a cobblestone-like monolayer of epithelial cells with an apical-basal polarity to dispersed, spindle-shaped mesenchymal cells with migratory protrusions;
- (2) changes of differentiation markers from cell-cell junction proteins and cytokeratin intermediate filaments to vimentin filaments and fibronectin;
- (3)

functional changes associated with the conversion of stationary cells to motile cells that can invade through the [extracellular matrix] ECM.

While individual examples of EMT can vary substantially, the ability to migrate and invade the ECM, as well as low E-cadherin and high vimentin expression, are considered key features of the EMT program. Important in development and silenced post-natally, EMT has also been implicated in carcinoma progression and metastasis (31, 34). Many studies, involving both cell culture and mice, have shown that originally epithelial cancer cells can acquire a mesenchymal phenotype. These cells that have undergone an EMT are commonly seen at the invasive front of tumors and are likely the cells that enter into the invasion-metastasis cascade as can be seen in Figure 1.2 (30, 35).

EMT's role in promoting cancer progression and metastasis may be a factor in contributing to acquired resistance to TKIs. Samples from patients with unknown mechanisms of resistance to TKIs have shown evidence of EMT, including changes consistent with a mesenchymal phenotype (12). Recently published studies have shown that the up-regulation of the AXL signaling pathway is both associated with EMT and results in acquired resistance to erlotinib (20). Additional studies have looked at other canonical EMT inducers, including TWIST1, and their roles in *EGFR* mutant lung cancer (36). Establishing causation between EMT and acquired resistance to TKIs would provide important mechanistic insights for many cancers, not just NSCLC. However the identification of a target within the EMT program is needed to develop therapies to combat this cellular program.



Nature Reviews | [Cancer](#)

**Figure 1.3. EMT is a dynamic process.** From Peinado, Olmeda & Cano. *Nature Reviews Cancer* (June 2007). Epithelial cells undergo a phenotypic change in which they lose cell-cell adhesion and can break through the basement membrane and enter the bloodstream through intravasation. The mesenchymal cells can undergo the opposite process, mesenchymal-epithelial transition (MET) and revert to the epithelial phenotype to colonize at distant sites.

One of the prototypical inducers of developmental and pathologic EMT is TWIST1, a basic helix-loop-helix (bHLH) transcription factor that has been shown to prevent oncogene-induced cell senescence and p53 mediated apoptosis, as well as to increase resistance to chemotherapy (37-39). Twist1 is essential for embryogenesis, with deletion being embryonic lethal and germ-line mutations, resulting in haploinsufficiency, leading to the development of Saethre-Chotzen syndrome, an inherited craniosynostosis condition that leads to abnormal limb development (38, 40). Typically undetectable in adult tissues, TWIST1 has been shown to be overexpressed in some cancers and that high expression has a strong correlation with cancers that are highly invasive and metastatic (37, 39, 41-47). *Twist1* is involved in EMT via down-regulation of key proteins that maintain an epithelial phenotype, like E-cadherin, and up-regulation of proteins that confer a mesenchymal phenotype, such as vimentin (37).

TWIST1 is amplified in many cancers, as can be seen in Figure 1.3 from the cBio database, not just lung cancer, indicating potential expanded benefit if TWIST1 is implicated in acquired resistance (48, 49). While data exists to link EMT to acquired resistance, there is little knowledge of how this occurs and a few studies have begun to link TWIST1 to acquired resistance to drugs, such as paclitaxel resistance in nasopharyngeal carcinoma cell lines (50). Interestingly, another study found that in hematologic cells, activation of Axl, already implicated in EMT and acquired resistance, induced expression of Twist1 (51). Whether such a relationship, or other interactions, occurs in *EGFR* mutant NSCLC is unknown, as is the direct role, if any, of TWIST1 in determining erlotinib acquired resistance.



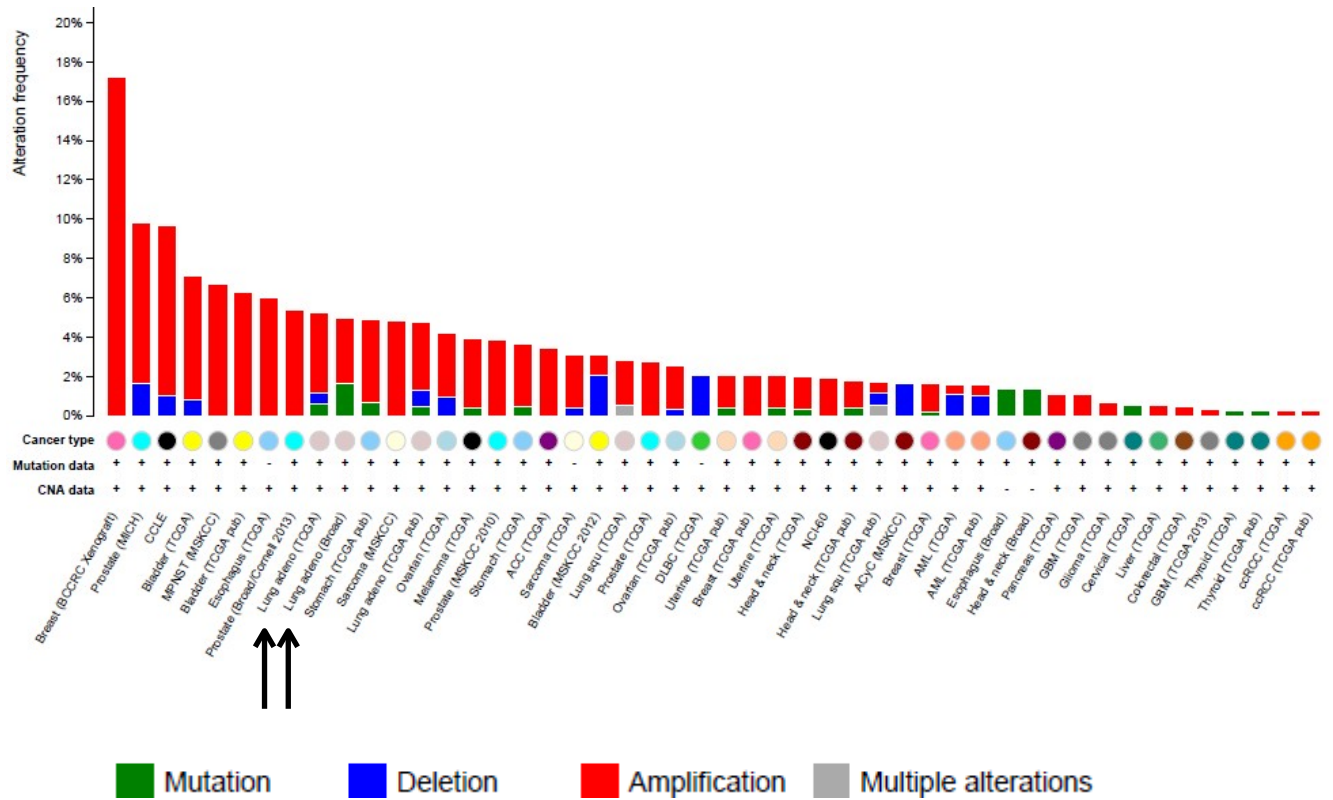


**Figure 1.4. Cross-cancer alteration summary for TWIST1 from cBio portal.** Genomic data from 105 cancer studies showing mutations, deletion, amplification and multiple alterations for TWIST1 across multiple cancers. In about 5% of lung cancers (indicated by arrows), TWIST1 amplification (red) is seen.

This thesis seeks to determine if Twist1, potentially through induction of the epithelial-mesenchymal transition (EMT), can cause resistance to erlotinib in *EGFR* mutant NSCLC and further starts to test potential Twist1 inhibitors for improved therapy. The first aim is to determine if TWIST1 can confer resistance to erlotinib and investigate the mechanisms of TWIST1-induced erlotinib resistance of lung cancer cell lines. This assumes that overexpression of TWIST1 will induce EMT and that in the *EGFR* mutant cell lines the overexpression is sufficient to induce resistance that can be observed through changes in cell viability. More importantly, the assumption is that it is EMT and not a different function of TWIST1, such as suppression of apoptosis, which is responsible for the resistance. However, development of an *in vitro* model is beneficial for teasing out a mechanism for the resistance and testing potential methods for overcoming the resistance.

The second aim is to determine if Twist1 will cooperate with mutant *EGFR* to induce lung tumorigenesis in an autochthonous lung tumor model. While *in vitro* models are helpful, having a transgenic mouse that has spontaneously arising lung cancer expressing both mutant *EGFR* and *Twist1* is far closer to modeling the actual human disease. The role of the tumor microenvironment, potentially essential to development of resistance, cannot be studied in cell culture; hence the necessity and benefit of a transgenic mouse model.

After developing the autochthonous lung tumor model, the third aim is to investigate the mechanisms of Twist1-induced erlotinib resistance *in vivo*. The resistant tumors can be isolated from mice and differences between genotypes and treatment groups characterized. Uncovering the changes induced by Twist1 expression and

erlotinib treatment could ultimately lead to determination of the underlying mechanism of resistance.

The final aim of this thesis seeks to test if compounds identified through Connectivity Mapping (CMap) can pharmacologically target Twist1 and inhibit tumor growth *in vivo*. Twist1 is commonly overexpressed in cancer and no current inhibitor exists. If a compound is found to inhibit Twist1, its use could improve therapy and in the setting of *EGFR* mutant NSCLC, could re-sensitize resistant cancers to conventional therapies. Together these studies will try to better understand a poorly characterized mechanism of resistance and attempt to find ways to overcome that resistance.

## **Chapter 2: Materials and Methods**

### **Cell lines**

The human NSCLC cell line HCC827 and embryonic kidney cell line HEK 293T were obtained from the American Type Culture Collection and grown in media as recommended. The human NSCLC cell lines, (11-18, PC9, HCC4006, HCC4011), were obtained from Dr. Katerina Politi and grown in media as recommended.

### **Lentiviral overexpression experiments**

293T cells were seeded ( $2.5 \times 10^6$  cells) in T25 flasks. Lentiviral particles were generated using a three-plasmid system and infected as per the TRC Library Production and Performance Protocols, RNAi Consortium, Broad Institute (52). Twenty-four hours after infection, cells were treated with 1  $\mu\text{g}/\text{mL}$  puromycin and passaged once 80% confluent.

### **Immunoblot analysis**

Cells or homogenized lung tissue were lysed on ice for 60 minutes in radioimmunoprecipitation assay buffer supplemented with protease and phosphatase inhibitors (Sigma-Aldrich) and clarified by centrifugation. Protein concentrations were determined by Pierce Micro BCA protein assay (Thermo Fisher Scientific). Equal protein concentrations of each sample were run on NuPAGE bis-Tris gels (Invitrogen) and electrophoretically transferred to polyvinylidene difluoride membranes. After being blocked with 5% dried milk in TBS containing 0.1% Tween 20, the filters were incubated with primary antibodies. The following primary antibodies were used: anti-EGFR (sc-03, Santa Cruz), -phospho-EGFR (3777, Cell Signaling), -AKT (9272, Cell Signaling), -phospho-AKT (4060, Cell Signaling), -ERK1/2 (9102, Cell Signaling), -phospho-

ERK1/2 (4370, Cell Signaling), -phospho-PAX (2541, Cell Signaling), -Twist1 (sc-81417, Santa Cruz), -GAPDH (FL-335, Santa Cruz). After washing and incubation with horseradish peroxidase (HRP)-conjugated anti-rabbit or anti-mouse IgG (Amersham), the antigen–antibody complexes were visualized by chemiluminescence (ECL detection system; Perkin Elmer).

### **Proliferation and viability assay**

Cells were seeded 5000 cells/well in a 96 well plate and allowed to attach overnight. The next day the cells were treated with erlotinib (0.001-100  $\mu$ M) for ~65 hours. At that point cell viability was assessed using CellTiter-Blue (Promega) and quantified on a SpectraMax M2e plate reader (Molecular Devices). Raw data were corrected for background luminescence, transformed ( $x=\log(x)$ ), and analyzed by nonlinear regression (log(inhibitor) vs. response with variable slope) in GraphPad Prism 5 to obtain IC<sub>50</sub> values, 95% confidence intervals, and R<sup>2</sup>. IC<sub>50</sub> was considered not determined if calculated as ambiguous by Prism. Transformed data were then normalized to untreated controls to generate log dose response curves. Results from representative experiments are shown.

### **Transgenic mice**

Mice were housed in groups of no more than five per cage with free access to food and water, under controlled light/dark cycles, in facilities with regulated temperature and humidity. Mice were randomly assigned to different experimental groups. All procedures were approved by the Institutional Animal Care and Use Committee of The Johns Hopkins University.

Inducible EGFR<sup>L858R</sup> and Twist1/EGFR<sup>L858R</sup> transgenic mice in the FVB/N inbred background were of the genotype: CCSP-rtTA/tetO-EGFR<sup>L858R</sup> (CE) CCSP-rtTA/tetO-EGFR<sup>L858R</sup>/Twist1-tetO-luc (CET). The CE mice were obtained from Dr. Katerina Politi. All the mice were weaned 3–4 weeks of age and then placed on dox at 4–8 weeks of age. Mice were left on DOX for 2-3 weeks before beginning treatment. The mice treated had similar levels of tumor burden per CT.

Erlotinib and dasatinib were purchased from Selleckchem (Houston, TX). For in vivo experiments, erlotinib was dissolved into a slurry in 0.5% methylcellulose, dasatinib was dissolved in 1% DMSO, 30% PEG, 1% Tween 80. The mice received 50 mg/kg erlotinib or vehicle via oral gavage, 30mg/kg dasatinib or vehicle via intraperitoneal injection daily, 6 days a week for 3 weeks.

### **Histology and immunohistochemistry**

Tissues were fixed in 10% buffered formalin for 24 h and then transferred to 70% ethanol until embedding in paraffin. Tissue sections 5 µm thick were cut from paraffin embedded blocks, placed on glass slides and hematoxylin and eosin (H&E) staining was performed using standard procedures (Johns Hopkins Histology Core). Antibodies used in our study: Twist1 (Santa Cruz), Ki-67 (Leica Biosystems), cleaved caspase 3 (Cell Signaling), vimentin (Abcam), and e-cadherin (Cell Signaling). Samples were dewaxed in xylene and rehydrated in a graded series of ethanols. Antigen retrieval was performed by 45 min rice-cooker irradiation in citrate-based Antigen Unmasking Solution (Vector Laboratories, Burlingame, CA, USA). Endogenous peroxidases were blocked in 3% hydrogen peroxide in methanol for 10 minutes. Non-specific binding was blocked with 2% bovine serum for 60 minutes or M.O.M. (Twist1). Primary antibodies were used at

appropriate dilutions (Twist1 at 1:200; vimentin and e-cadherin at 1:400; cleaved caspase 3 at 1:500; and Ki-67 at 1:2000) and sections incubated overnight at 4 degrees Celsius. Secondary incubation was done using PowerVision Poly-HRP anti-rabbit IgG (Leica Biosystems) or using M.O.M. for Twist1 (Vector Laboratories). Visualization was performed using DAB substrate kit for Peroxidase (Vector Laboratories). Sections were counterstained with Gill's hematoxylin (Vector Laboratories) and slides were mounted in aqueous mounting media (Vector Laboratories).

### **PathScan RTK antibody array kit**

The PathScanRTK signaling array kit containing 39 fixed antibodies against phosphorylated forms of kinases and key signaling proteins by the chemiluminescent sandwich ELISA format was used per manufacturer's direction (Cell Signaling Technologies). Images were analyzed with ImageJ (<http://rsbweb.nih.gov/ij/>) by loading the image as a gray scale picture. Each kinase array dot was manually selected, and an average intensity for each kinase was calculated. Normalization within one stimulation experiment was done by subtracting the intensity of the negative control dot from each value. For comparison of different stimulation conditions, sets were normalized so that the positive controls had equal intensities.

### **Microarray data acquisition and analysis**

Microarrays were performed using GeneChip WT cDNA Synthesis and Amplification Kit and WT Terminal Labeling Kit (Affymetrix, Santa Clara, CA). RNA was isolated by the Johns Hopkins Medical Institution Deep Sequencing and Microarray Core Facility. The labeled ssDNA was hybridized to the GeneChip Mouse Gene 1.0 ST Array (Affymetrix), washed with the Fluidics Station 450, and array scanning was

conducted as previously described (53). Arrays were normalized using the Robust Multichip Average in the oligo Bioconductor package at the transcript level (54). Genes and gene sets with Benjamini-Hochberg (55)  $P < 0.05$  were considered statistically significant. Gene set enrichment analysis (GSEA) was performed using the C2 Curated Gene Sets collection from the Molecular Signature Database 3.0 and statistical comparisons by Fisher exact test. Additionally, data were analyzed through the use of QIAGEN's Ingenuity® Pathway Analysis (IPA®, QIAGEN Redwood City, [www.qiagen.com/ingenuity](http://www.qiagen.com/ingenuity)).



## Chapter 3: Characterization of TWIST1 mediated acquired resistance to Erlotinib in EGFR mutant lung cancer cell lines.

### Section 3.1: Results

To explore the role of TWIST1 in resistance to EGFR targeted therapy, we stably overexpressed TWIST1 in the erlotinib sensitive *EGFR* mutant human cell lines, HCC827, 11-18, PC9, HCC4006, and HCC4011 (Fig. 3.1A). Both of the most common EGFR TKI sensitizing mutations, the exon 19 deletion (PC9, HCC827, HCC4006) and the L858R mutation (HCC4011, 11-18) were represented. TWIST1 was ectopically expressed in these cell lines and westerns were performed to assess the effect of TWIST1 overexpression on EGFR and downstream phosphorylation both in the presence and absence of erlotinib treatment. Not unexpectedly, an increase in pAKT is seen with TWIST1 expression and erlotinib treatment in HCC4006, HCC4011 and PC9. Additionally, in PC9, phospho-ERK1/2 levels are slightly higher in the *TWIST1* expressing line, compared to vector control, with erlotinib treatment. In HCC4011, the level of phospho-EGFR is decreased with the combination of TWIST1 expression and erlotinib treatment, compared to vector control. Interestingly, the level of phospho-EGFR in HCC827 was decreased by the expression of TWIST1 alone compared to control, both at baseline and with erlotinib treatment (**Fig. 3.1B**).

Having seen the change in downstream signaling components after erlotinib exposure for only 24 hours, we utilized MTS assays to assess the effect of TWIST1 expression on erlotinib sensitivity and resistance. Interestingly, varying degrees of acquired resistance to erlotinib was observed with TWIST1 overexpression in all cell lines, after 72 hours of erlotinib exposure. HCC4011 showed the greatest decrease in sensitivity to erlotinib as a result of *TWIST1* overexpression. Conversely, two of the cell lines, 11-18 and PC9, showed a slight increase in erlotinib sensitivity with TWIST1 expression (**Fig. 3.2**). While these data demonstrate a trend towards TWIST1 expression conferring resistance *in vitro*, the results were not conclusive as different cell lines showed varying results.

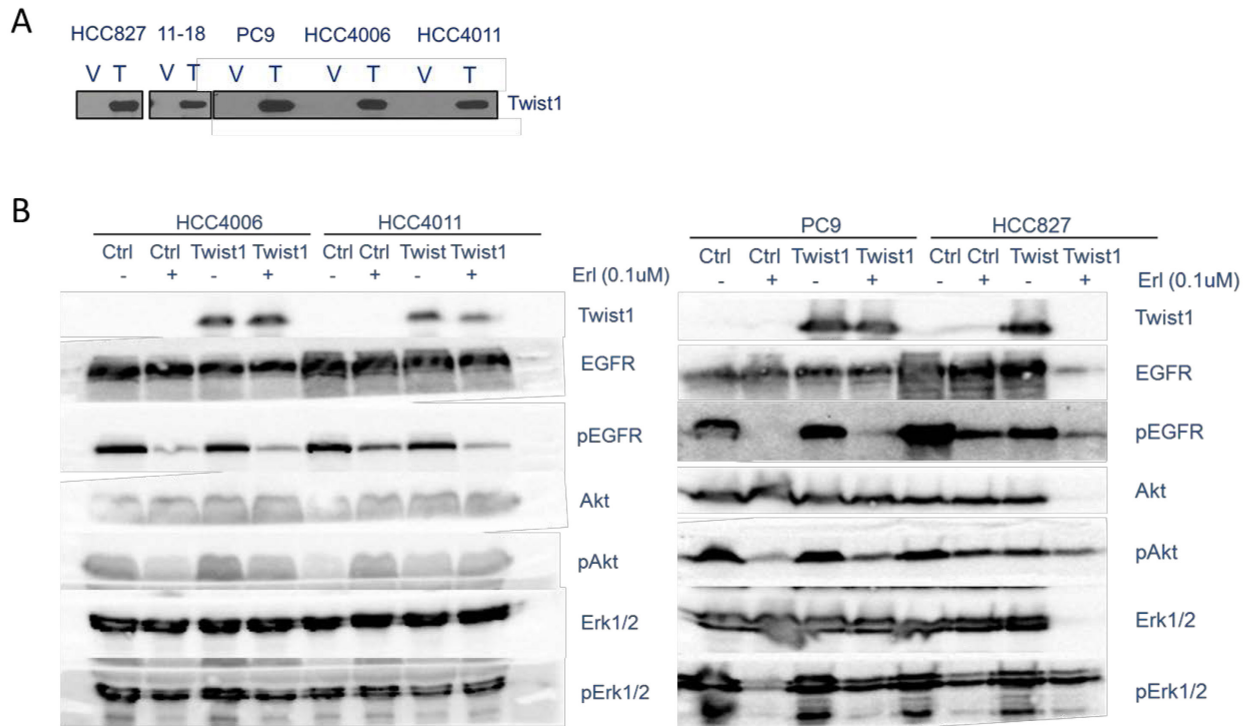


**Figure 3.1. Overexpression of TWIST1 alters levels of phosphorylation downstream of EGFR in vitro.** (A) Five EGFR mutant cell lines were infected with TWIST1 or vector control. (B) Western showing levels of proteins downstream of EGFR with TWIST1 overexpression, plus or minus erlotinib treatment for 24 hours, in the *EGFR* mutant cell lines HCC4006, HCC4011, HCC827 and PC9. In HCC4006, an increase in pAkt is seen with TWIST1 expression and erlotinib treatment. A similar increase is seen in HCC4011, as well as a decrease in pEGFR with TWIST1 expression and erlotinib treatment. The cell line PC9, shows an increase in levels of pAkt and pErk1/2 with TWIST1 expression in the presence of erlotinib. A decrease in pEGFR with TWIST1 expression is seen in HCC827, with and without erlotinib treatment.

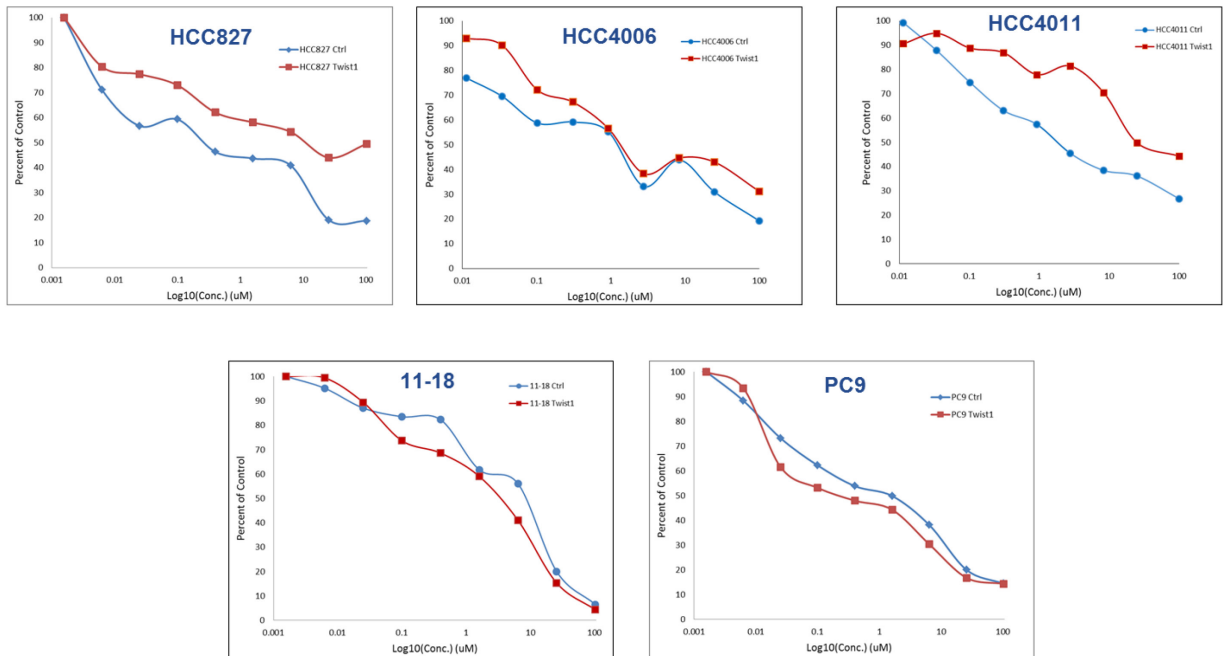


**Figure 3.2. Overexpression of TWIST1 confers erlotinib resistance in a subset of EGFR mutant cell lines.** MTS assays demonstrating varying degrees of growth inhibition of erlotinib in HCC827, HCC4006, HCC4011, 11-18 and PC9 vector control and TWIST1 EGFR mutant cell lines following treatment with erlotinib at 72 hrs. In two of the cell lines, 11-18 and PC9, *TWIST1* expressing lines actually appear more sensitive to erlotinib. Similar viability is seen between control and TWIST1 lines in HCC4006, while modest decreases in sensitivity are seen in HCC827 and HCC4011.

### Section 3.2: Discussion

A common method for creating resistant cell lines is sequential exposure to higher drug doses (56), however here overexpression of a single protein appears sufficient to induce changes potentially demonstrating resistance. Previous studies have shown that when drug resistant lines are created from the parental *EGFR* mutant cell lines, the mechanism of resistance differs between cell lines and even between different clones from the same cell line (57). While TWIST1 expression did result in changes in levels of phosphorylation downstream of EGFR, both in the absence and presence of erlotinib, the changes varied between cell lines. Additionally, a change in phosphorylation levels of any proteins looked at did not necessarily equate to a change in cell viability in the short term viability assays and thus an alteration in sensitivity to erlotinib.

The lack of a correlation between changes in downstream signaling and change in viability indicates that TWIST1 overexpression is inducing resistance to erlotinib in a cell type specific manner. While all the cell lines possessed an erlotinib sensitizing *EGFR* mutation, the other characteristics, in all likelihood, differed greatly. Some of the cell lines may innately be more mesenchymal or epithelial or have different genetic modifications or mutations before overexpression of TWIST1. Characterizing the differences between the cell lines by determining baseline levels of epithelial/mesenchymal markers as well as checking if other mutations or modifications exist could potentially help explain the variety of changes seen with TWIST1 overexpression and erlotinib exposure.

Several other possible explanations for the lack of consistency between Westerns, which were done at 24 hours and the viability assays, where cells were treated with

erlotinib for 65 hours or more, exist. A very plausible explanation is that some sort of 3D structure is required for resistance. One of the cell lines, HCC4011, tended to form a spherical structure in cell culture. The viability assay caught the change in erlotinib sensitivity for this cell line because the longer time period allowed the cells to form the 3D structure. Another potential explanation is that there are signals from the tumor microenvironment that mediate the resistance. Several studies have been published showing that cell-adhesive interactions, such as activation of focal adhesion kinase (FAK) and SRC, within the tumor niche result in resistance (58, 59). These changes in the microenvironment could be either as a result of TWIST1 expression or result in TWIST1 expression. Ultimately, further investigation is required to develop an *in vitro* model of TWIST1-mediated erlotinib resistance. Repeating these experiments on collagen I or other extracellular matrix protein coated plates could result in very different data if, in fact, signals from the extracellular matrix is required for the development of resistance.

### **Section 3.3: Conclusions**

The overexpression of TWIST1 alone in *EGFR* mutant cell lines appears to induce resistance to erlotinib in a cell type specific manner. One explanation for the failure of consistent induction of erlotinib resistance could be that the mechanism is not cell autonomous and requires the involvement of the tumor microenvironment or other interactions that simply are not present in cell culture. Other possibilities include baseline differences in the cell lines as well as additional mutations present in some lines but not others. Further experimentation is required to determine if an *in vitro* model can be developed using these cell lines.

## Chapter 4: Creation and Characterization of an Autochthonous *EGFR* Mutant Lung Tumor Model

### Section 4.1: Results

Transgenic mice are often used to study human cancers and both *EGFR*<sup>L858R</sup> and *Twist1* inducible mouse models have been created (39, 60). Previous studies have looked at the effect of Twist1 overexpression on mutant *Kras* tumorigenesis (39); however the interaction between Twist1 and mutant *EGFR*, especially in the context of acquired resistance, has yet to be closely studied. We therefore utilized two doxycycline inducible lung specific transgenic mouse models, *CCSP-rtTA/tetO-EGFR*<sup>L858R</sup> (CE), expressing human EGFR and *CCSP-rtTA/Twist1-tetO<sub>7</sub>-luc* (CT), expressing mouse Twist1. We crossed the two lines to create triple transgenic mice, *CCSP-rtTA/tetO-EGFR*<sup>L858R</sup>/*Twist1-tetO<sub>7</sub>-luc* (CET) (**Fig. 4.1A**). Having created this new model, we sought to assess the effect of Twist1 overexpression in the absence of treatment. Cohorts of CE and CET mice, aged 4-8 weeks, were administered doxycycline in the drinking water to turn on the transgenes. After 4 weeks, a point by which CE mice have developed tumors (60), mice were sacrificed and necropsies performed. Upon comparison of H&E sections from CE and CET mice by a veterinary pathologist, it was determined that CET tumors are more anaplastic and have larger, more irregular nuclei (**Fig. 4.1B**). The lesions from both genotypes were more diffuse rather than discrete tumors, as had been previously published for the CE model (60). Histologic changes are visible in CE mice after only 2 weeks of doxycycline administration (60), and we have previously shown that Twist1 expression accelerates mutant *Kras* tumorigenesis (39). After 4 weeks on doxycycline, when tumor burden is compared between CE and CET mice, there is no apparent difference (**Fig. 4.1C**). While variability exists within each genotype, as to the disease

burden, the total tumor burden is similar when compared across both CE and CET genotype (**Fig. 4.1D**). This suggests that despite a more aggressive or anaplastic appearance in the CET tumors, both genotypes develop tumors at approximately the same rate.

To further characterize the novel CET mouse model, we looked at levels of epithelial and mesenchymal markers, since Twist1 is an inducer of EMT. We immunostained lung sections from both CE and CET mice with antibodies for e-cadherin, an epithelial marker, and vimentin, a mesenchymal marker. There was no distinguishable difference in levels of either marker between CE and CET mice (**Fig. 4.2A**). In previous studies, Twist1 has been shown to impact the proliferation rate of tumor cells as well as apoptosis levels (61, 62). We looked at the levels of proliferation through immunohistochemistry with an antibody for Ki-67 and apoptosis with an antibody for cleaved caspase 3. The overexpression of Twist1 in CET mice decreased proliferation rates, as measured by Ki-67 IHC, in comparison to CE mice (**Fig. 4.2B**). There was no apparent effect on apoptosis with Twist1 expression (**Fig. 4.2C**). While there is no evidence of tumor cells undergoing EMT, Twist1 can decrease proliferation in the short term, a characteristic often seen as a result of EMT-inducing transcription factors (61).



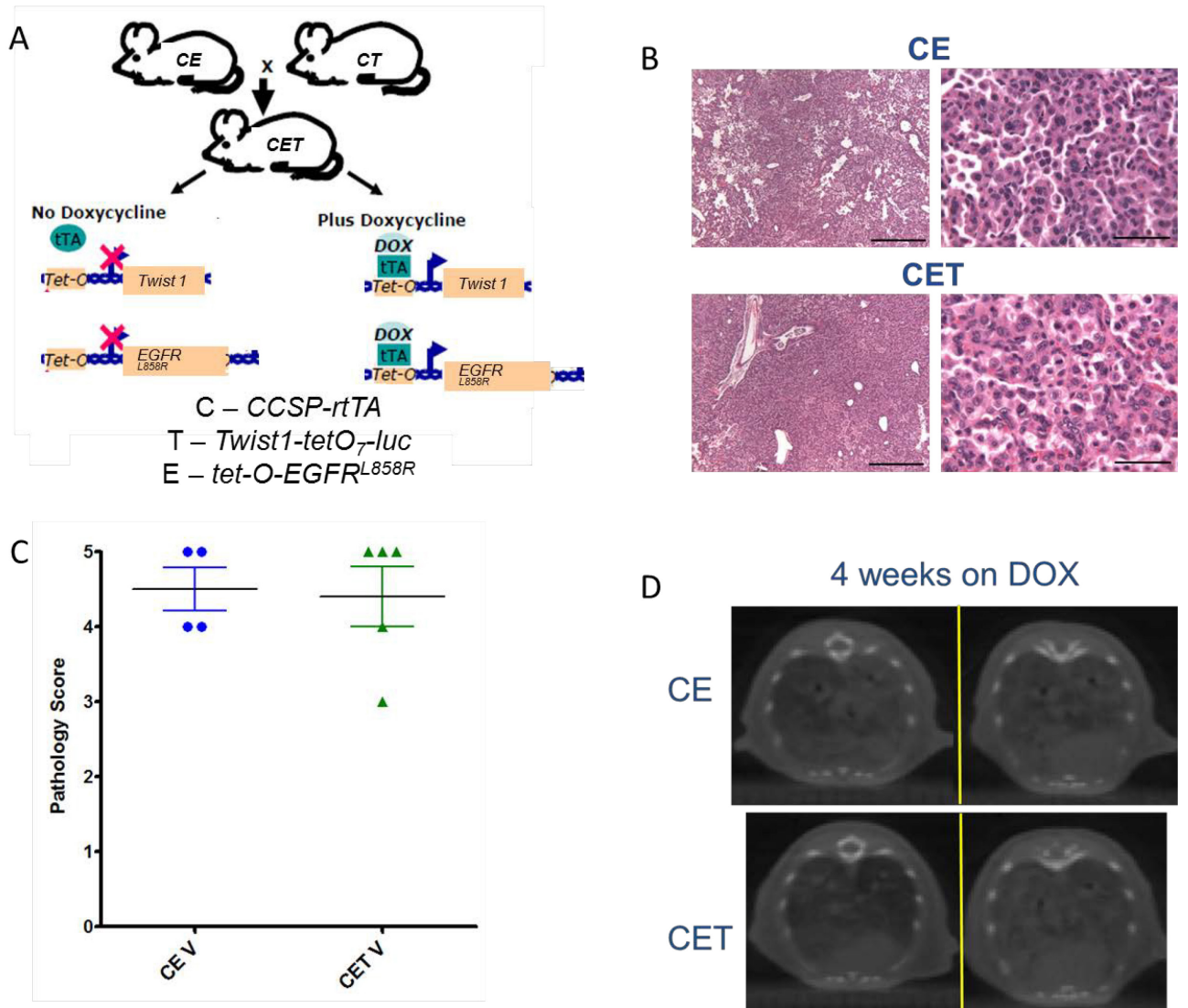


**Figure 4.1. Generation and characterization of a novel Twist1 overexpressing, mutant EGFR autochthonous lung tumor mouse model.** (A) Crosses (CE×CT) to produce CCSP-rtTA/EGFR<sup>L858R</sup>/Twist1-tetO<sub>7</sub>-luc (CET) mice. (B) H&E images from lung tissue of CE and CET mice. CET histology was more anaplastic with larger, more irregular nuclei. Lesions in both genotypes are more diffuse rather than discrete tumors. Black bars equal 500 and 50  $\mu$ m. (C) Comparison of tumor burden, as percent of lung affected, between CE and CET untreated mice. Mice were on doxycycline for 4 weeks then sacrificed. (D) CT images from CE (upper) and CET (lower) mice on doxycycline for 4 weeks. As evidenced from the images, varying levels of tumor burden can be seen within a genotype, however the level is comparable between genotypes. CT images are non-invasive and based on density; the denser areas, like bone, appear white, while the air space is black. The mice are lying on their stomach with noses pointed forward.

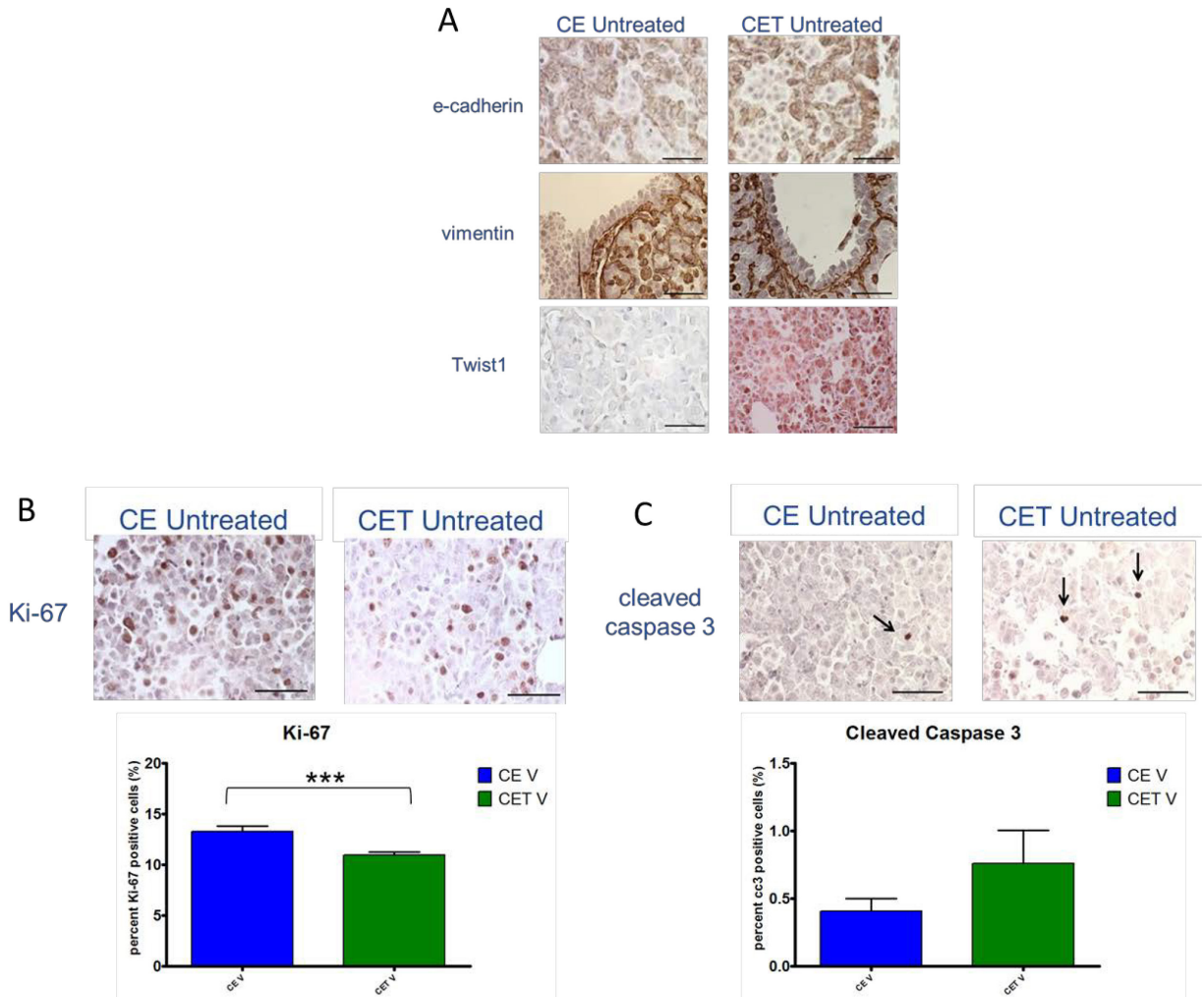


**Figure 4.2. Generation and characterization of a novel Twist1 overexpressing, mutant EGFR autochthonous lung tumor mouse model.** (A) Similar levels of e-cadherin and vimentin staining in CE and CET mice, with CET mice expressing Twist. (B) Decreased proliferation in CET mice compared to CE mice as determined by Ki-67 staining.  $P < 0.0005$ . (C) Similar levels of apoptosis in CE and CET mice using cleaved caspase 3 IHC. For B-G,  $n = 4$  mice per genotype, black bars equal 50  $\mu\text{m}$ .

## Section 4.2: Discussion and Conclusions

In this study, the development of a novel mouse model is described. While both the CE and CT models have previously been described (39, 60) this is the first characterization of the cross between the two genotypes, the CET mouse. This model was created to model what could be a subset of acquired resistance cases to EGFR TKIs that have undergone an EMT. Having previously seen that Twist1 accelerates mutant *Kras* lung tumorigenesis (39), the finding that there does not appear to be any acceleration in the setting of mutant *EGFR* is surprising. The CE mice do develop tumors much quicker than the CR mice (39, 60) so it is possible that earlier CT scans or a more detailed imaging method would be required to capture any differences in tumorigenesis. An ongoing experiment is studying the difference in overall survival between CE and CET mice; it is expected that CE mice will live much longer, even in the absence of treatment, than CET mice.

The lung tumors in the CET mice are more anaplastic than those seen in CE mice, with larger more irregular nuclei. This is consistent with reports of cancers expressing Twist1 being more aggressive (63). Both genotypes display diffuse hyperplasia instead of discrete tumors, which is similar to the disease seen in some *EGFR* mutant NSCLC in humans. Additional characterization of the histology of the CET mice is needed. Mice were sacrificed after being on doxycycline for only 4 weeks, however it takes, on average, more than 4 weeks for CE mice to develop multifocal invasive adenocarcinomas (60). Mice would need to be sacrificed at distinct time points, after 4 weeks, to compare the histology of CET versus CE and determine what, if any, effect Twist1 has on the

development of adenocarcinoma. Additionally, PET could be used to look at differences in metabolism induced by Twist1 overexpression.

Initial characterization demonstrated that overexpression of Twist1 was not sufficient to induce any changes in levels of e-cadherin or vimentin, at least as assessed by IHC. Every case of EMT is unique, however, so the similar levels of epithelial and mesenchymal markers between CE and CET mice is not completely unexpected. The decrease in proliferation in CET mice in the absence of treatment is interesting and could benefit from further investigation. Additional characterization of the CET mouse is definitely warranted, as this is a novel transgenic mouse model and the interaction between Twist1 and mutant *EGFR* for lung tumorigenesis is apparently distinct from that of Twist1 and mutant *KRAS*. This novel mouse model may prove to be useful in studying targeted therapy resistance and examining the role of Twist1 in the *EGFR* mutant subset of NSCLC.

## Chapter 5: Investigation of the Mechanisms of Twist1-induced Erlotinib Resistance in a mouse model of EGFR Mutant Lung Cancer

### Section 5.1: Results

#### ***Twist1* expression results in erlotinib resistance.**

After characterizing the novel CET mouse model in the absence of drug treatment and demonstrating that Twist1 overexpression does not appear to accelerate *EGFR* mutant tumorigenesis, we wanted to investigate whether Twist1 expression would induce resistance to the EGFR TKI erlotinib *in vivo*. As previously described, upon administration of erlotinib to CE mice, the tumors regress and in some cases, a complete response occurs (60). In order to compare CE and CET mice tumor responses and overall survival, all mice were put on doxycycline, to turn on gene expression, by 8 weeks of age, and allowed to develop tumors for 3 weeks. Both CE and CET mice had similar levels of tumor burden prior to the start of treatment. At that time point, treatment day 0, all mice were scanned by CT and this scan was used as the baseline. The mice were treated for 3 weeks with erlotinib and scanned by CT each week (**Fig. 5.1A**). When baseline scans were compared to scans from after 3 weeks of erlotinib treatment, tumor regression was clearly visible in CE mice, while CET mice showed an increase in tumor burden (**Fig. 5.1B**). All scans were assessed and tumor burden graded on a scale of 0 (no tumor visible) to 5 (lungs completely filled with tumor). Based on the tumor burden change from the beginning to the end of treatment, a majority of CE mice demonstrated no disease progression, with no progression including complete and partial responses as well as stable disease. Conversely, over half of the CET mice had tumor progression over the three weeks of treatment (**Fig. 5.1C**). When looking at regression, a decrease in tumor burden grading, two-thirds of CE mice regressed. Only a quarter of CET mice

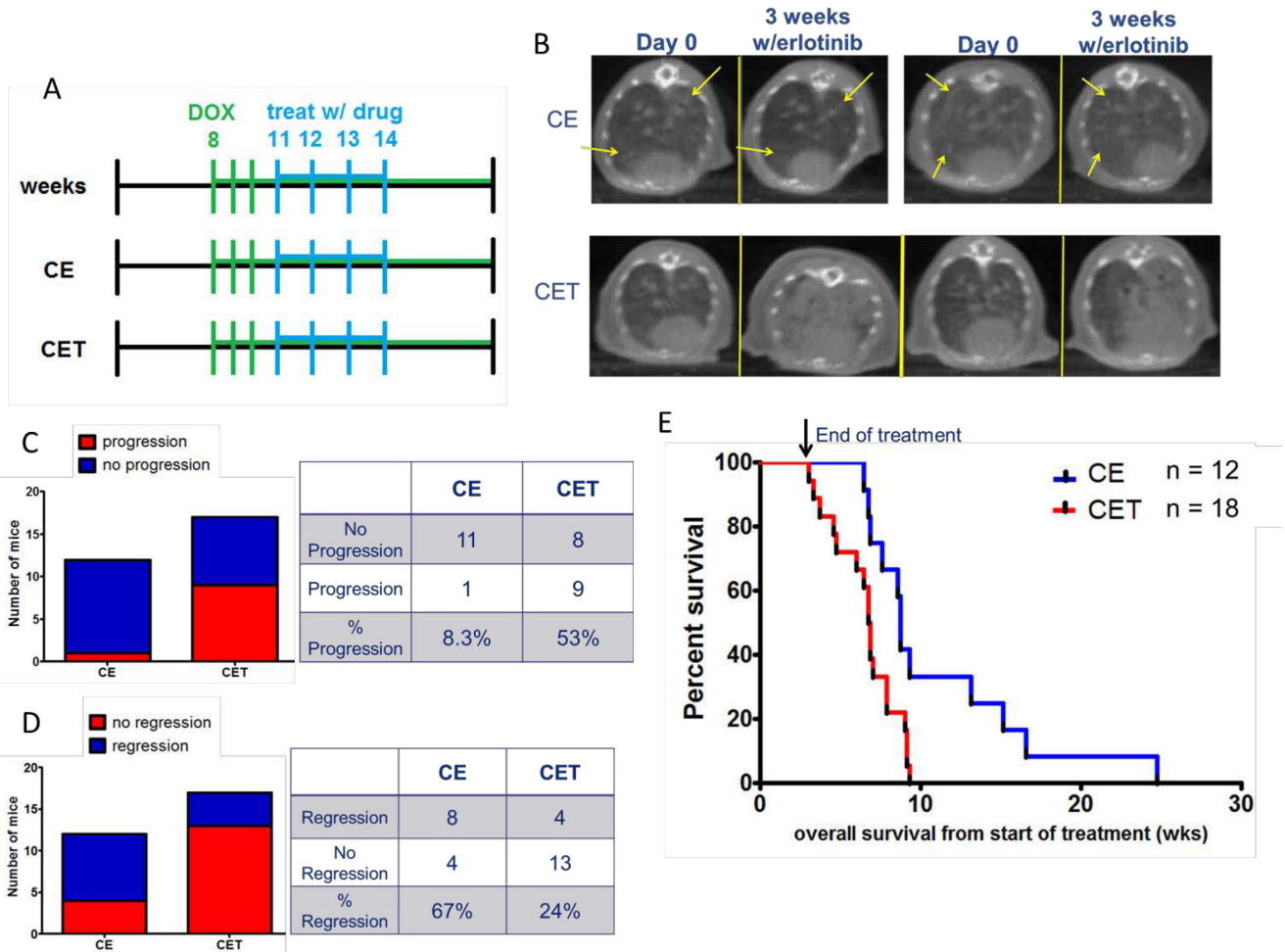


**Figure 5.1 Twist1 expression results in erlotinib resistance.** (A) Treatment schema for CE and CET mice erlotinib treatment. Mice are put on doxycycline, inducing EGFR<sup>L58R</sup> and Twist1 transgene expression, around 8 weeks of age and allowed to develop tumors for 3 weeks. Mice are scanned at the beginning of treatment, week 11, and each week thereafter until the end of treatment. Mice are treated with 50 mg/kg erlotinib by oral gavage 6 days a week for 3 weeks (weeks 11-14). (B) CT images from baseline and after 3 weeks of erlotinib treatment for CE and CET mice. CE mice show a decrease in tumor burden at the end of treatment compared to day 0. CET mice show a drastic increase in tumor burden despite 3 weeks of treatment. (C) Tumor burden, as visualized by CT image, was graded on a scale of 0 (no tumor) to 5 (lungs filled with tumor) at day 0 and the end of treatment. No progression was considered a complete or partial response as well as stable disease. Only 1 CE mouse demonstrated disease progression, while over half of the CET progressed despite erlotinib treatment. (D) Regression was a decrease in tumor burden grade at 3 weeks compared to baseline. Two-thirds of CE mice regressed, while only one quarter of CET mice showed regression. (E) Kaplan-Meier overall survival from beginning of treatment. Median survival for CE mice was 8.7 weeks, for CET mice was 6.8 weeks.

demonstrated regression based on CT scans (**Fig. 5.1D**). After the 3 weeks of treatment, mice were monitored for weight loss, lethargy and other signs indicating a need for euthanasia or until mice died naturally. CET mice median overall survival time, from the beginning of treatment, was 6.8 weeks, while CE mice lived a median of 8.7 weeks (**Fig. 5.1E**). Importantly, we have demonstrated that Twist1 does not lead to an increased tumor burden in the EGFR mice so an increased tumor burden cannot explain this decrease in overall survival (**Fig. 4.1**) These data demonstrate that expression of TWIST1 in CET mice induces resistance to erlotinib as seen by CT scans of lung tumor burden as well as by decreased overall survival time.

To confirm the differences seen by CT, a cohort of CE and CET mice were treated with erlotinib for 1 week and the tumor histology assessed by a veterinary pathologist. While partial and complete responses were seen in CE mice, only partial and no responses occurred in the CET mice (**Fig. 5.2A**). Some of the CET mice demonstrated adenoma, though no adenocarcinoma was seen in the histology (**Fig. 5.2B**). Tumor burden, with the score reflecting the percent affected lung in each animal (0 meaning no hyperplasia and 5 meaning >75% of the lung is affected), was determined from the H&E slides by a veterinary pathologist. The tumor burden difference between CE and CET mice treated with erlotinib was not statistically significant, however there is an apparent trend towards CET mice having greater tumor burden (**Fig. 5.2C**).

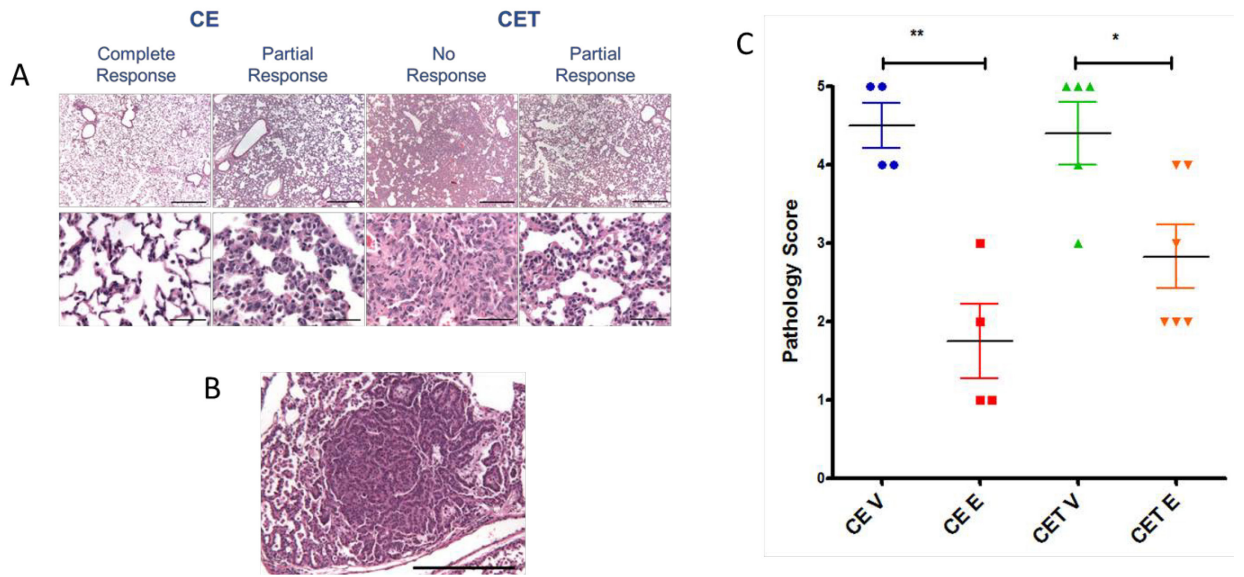


**Figure 5.2. Twist1 expression alters tumor burden and response to erlotinib treatment.** (A) H&E images showing comparison of responses seen in CE and CET mice after only 7 days of erlotinib treatment. Black bars equal 500 (top) and 50 (bottom)  $\mu\text{m}$ . (B) Representative image of adenoma in a CET mouse. Black bar equals 250  $\mu\text{m}$ . (C) Pathology scores indicating tumor burden as percent of total lung affected.



### **Characterization of Twist1 induced resistance.**

Having demonstrated that expression of Twist1 leads to erlotinib resistance in the autochthonous mouse model, the mechanism of how Twist1 conveys this resistance remains unknown. Since Twist1 is one of the key mediators of EMT, the tumor cells could be undergoing this phenotypic change. However staining for e-cadherin and vimentin showed no change with Twist1 expression, with or without erlotinib treatment (**Fig. 5.3A**). Overexpression of Twist1, in the absence of treatment, decreased proliferation rates, as seen by Ki-67 levels. However, there was no significant difference between proliferation levels in CE and CET mice (**Fig. 5.3B & 5.3C**). Interestingly, when the amount of apoptosis was assessed through staining for cleaved caspase 3, the levels of apoptosis were decreased in CET erlotinib treated tissues compared to CE erlotinib treated tissues (**Fig. 5.3D & 5.3E**). This data suggests that while the level of proliferation is unchanged in the presence of erlotinib, the amount of apoptosis decreases with Twist1 expression and erlotinib treatment.

Many resistance mechanisms to targeted therapies are the result of amplified signaling through a parallel or complimentary signaling pathway (3, 12, 64, 65). Twist1 could potentially be indirectly activating an alternative to the EGFR signaling cascade, leading to resistance. To determine if other pathways were upregulated, we utilized a RTK Signaling Antibody Array Kit from Cell Signaling. The output indicated if there were increased or decreased phosphorylation levels of the RTKs and signaling nodes represented by antibodies on the slide. Remarkably, several kinases/signaling nodes showed differential phosphorylation when compared between genotypes and treatment groups (**Fig. 5.4A**). The highest signal seen in the CET erlotinib treated samples were

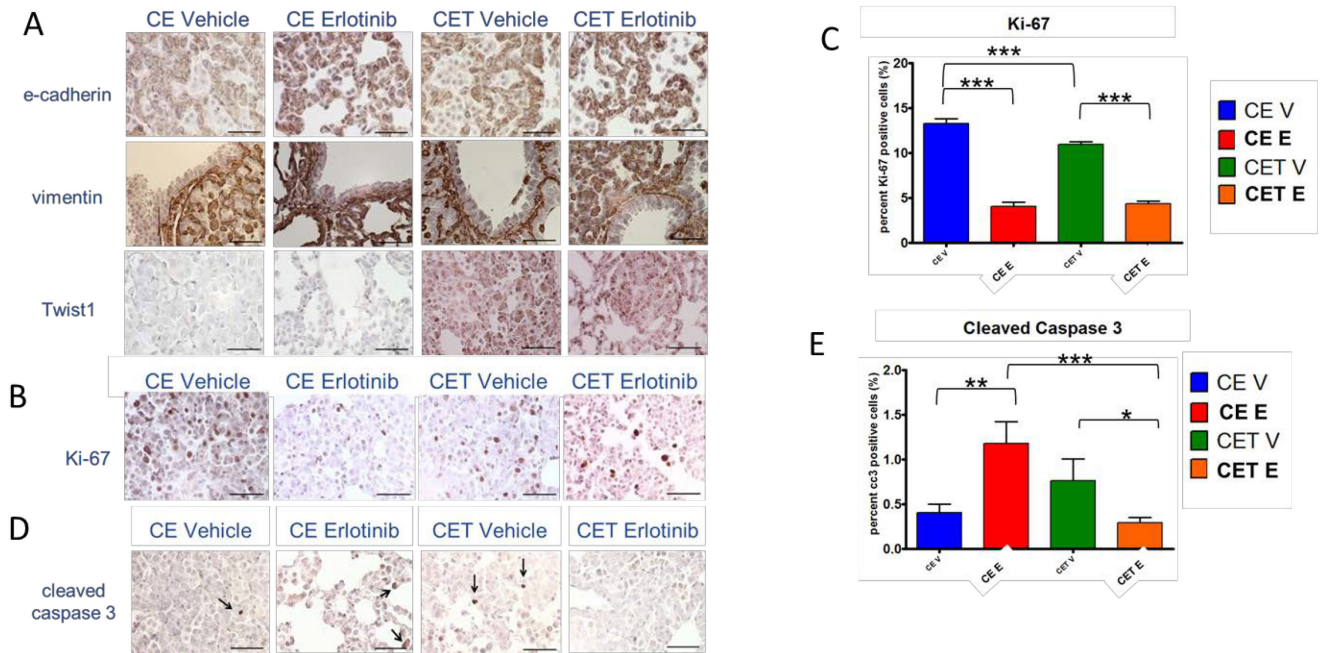


**Figure 5.3. Characterization of Twist1 induced erlotinib resistance.** (A) Similar levels of e-cadherin and vimentin staining in CE and CET mice with and without erlotinib treatment, with CET mice expressing Twist. (B) Representative images of Ki-67 staining and quantification (C) of staining showing a decrease in proliferation to similar levels with erlotinib treatment in both CE and CET mice. (D) Representative images of cleaved caspase 3 staining and quantification (E) showing a decrease in apoptosis in CET compared to CE mice with erlotinib treatment. \*  $p < 0.05$ , \*\*  $p < 0.005$ , \*\*\*  $p < 0.0005$ . Black bars in A, B, D equal to 50  $\mu\text{m}$ .

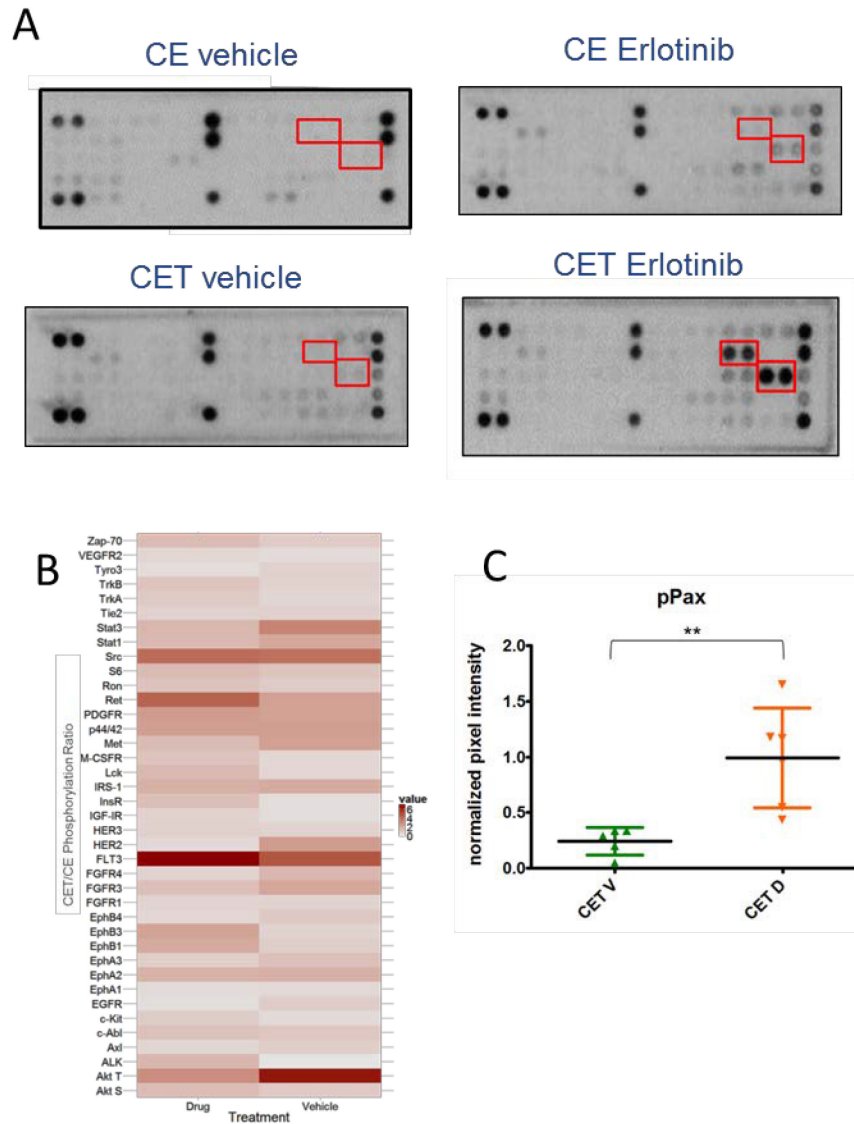


**Figure 5.4. Twist1 expression alters phosphorylation levels of RTKs and signaling nodes.** (A) Representative images from RTK antibody array showing increased phosphorylation of AKT serine 473 (left box) and Src (right box) in CET erlotinib treated sample compared to CE erlotinib treated. (B) Heat map showing phosphorylation ratio of CET to CE samples for all RTKs and signaling nodes represented on antibody array. (C) Quantification of western looking at levels of phospho-Paxillin in CET mice treated with vehicle and erlotinib. Levels were increased in drug treated CET mice.

from Src and serine 473 on Akt. A heat map was created comparing the phosphorylation ratio of CET to CE samples (**Fig. 5.4B**). Of the potential targets identified from the heat map, Src was the most appealing, as data from other groups indicated a role for the Src family in EMT related drug resistance (66). Additionally, there have been some studies showing TWIST1 can upregulate Src and that Src can increase TWIST1 levels (67, 68). When we looked at paxillin, a direct phosphorylation target of Src, we saw elevated levels of phosphorylated paxillin in CET mice with erlotinib treatment (**Fig. 5.4C**). This further supported the hypothesis that Src was involved with the Twist1-mediated erlotinib resistance.

#### **Validation and investigation of Src target.**

One of the potential mechanisms to overcome or prevent acquired resistance is the combination of targeted therapies. Prior studies have demonstrated success with this method in erlotinib acquired resistance (69-72). Having identified Src as being differentially phosphorylated through the antibody array, we sought to target Src in combination with erlotinib to attempt to overcome the resistance seen in CET mice. We administered two different doses, low (10 mg/kg) and high (30 mg/kg), of dasatinib, a Src family, as well as Bcr-Abl, inhibitor, alone and with erlotinib to CET mice in a short pilot experiment. When the mice were sacrificed after only 5 days of treatment, significant reduction in tumor burden was seen in the mice administered 30 mg/kg dasatinib and the standard 50 mg/kg erlotinib, in comparison to the other treatment groups. (**Fig. 5.5A & 5.5B**). The level of e-cadherin and vimentin staining was fairly uniform across treatment groups (**Fig. 5.5C**). Interestingly, the level of proliferation decreased with the combination treatment, in comparison to either single therapy, as indicated by Ki-67

staining (**Fig. 5.5D & 5.5E**). To confirm we were achieving Src inhibition, we looked at the levels of the direct target paxillin and saw a decrease in phosphorylation levels with combination treatment (**Fig. 5.6A**). We also saw decreases in phosphorylation of AKT, demonstrating the downstream effects of erlotinib and dasatinib combination treatment (**Fig. 5.6B**).

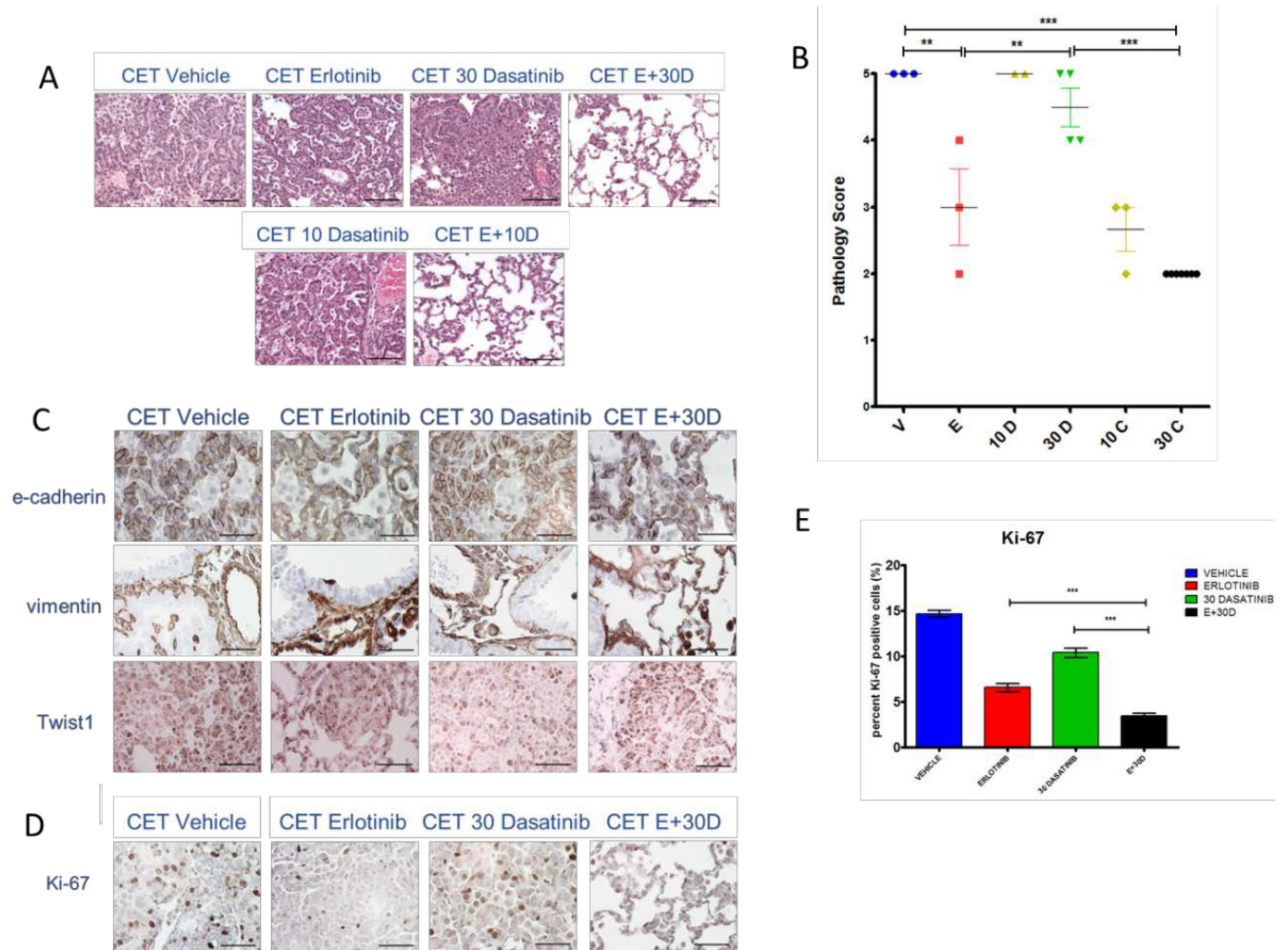


**Figure 5.5. Validation and Investigation of Src target.** (A) Representative H&E images from each treatment group showing a decrease in tumor burden in 30 mg/kg dasatinib and 50 mg/kg erlotinib combination group. Black bars equal 100  $\mu$ m. (B) Pathology scores reflecting percent of lung affected. (C) Similar levels of e-cadherin, vimentin and Twist1 by IHC staining between treatment groups. (D) Representative images of Ki-67 IHC and quantification (E) demonstrating a decrease in proliferation with combination treatment. \*  $p < 0.05$ , \*\*  $p < 0.005$ , \*\*\*  $p < 0.0005$ . Black bars in C, D equal 50  $\mu$ m. For A-E, vehicle  $n = 2$ , erlotinib  $n = 2$ , 10mg/kg dasatinib  $n = 2$ , 30mg/kg dasatinib  $n = 2$ , erlotinib + 10mg/kg dasatinib  $n = 3$ , erlotinib + 30mg/kg dasatinib  $n = 3$ .

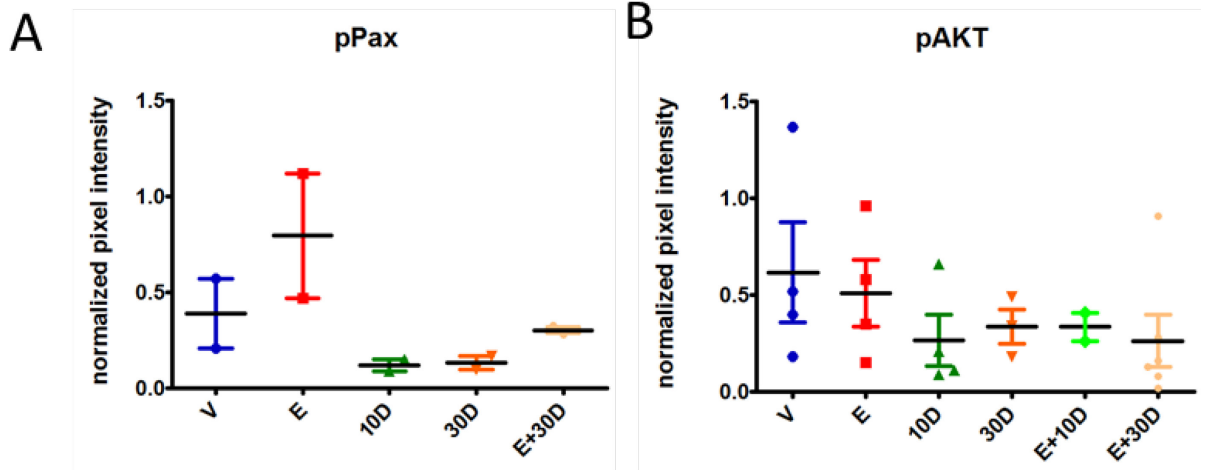


**Figure 5.6. Combination treatment decreases downstream phosphorylation.** Quantification of Western using lung lysates from CET mice showing a decrease in phospho-Paxillin (A) and phospho-Akt (B) with combination treatment.

**Combination treatment with erlotinib and dasatinib overcomes resistance resulting from *Twist1* expression.**

The results from the short term experiment treating CET mice with erlotinib and dasatinib indicated that targeting Src was able to overcome Twist1 mediated erlotinib resistance. The effect of combination treatment on tumor burden and overall survival, clinically relevant factors, was not determined in these short term experiments.. Thus, we treated cohorts of CET mice with vehicle, erlotinib alone, 30 mg/kg dasatinib alone, or combination of erlotinib and dasatinib, for 3 weeks, as had been previously done in CE and CET mice with erlotinib. Baseline CT scans were taken at the beginning of treatment and compared to scans from the end of 3 weeks of treatment. Reduction in tumor burden was visible by CT and seen in a majority of combination treated mice (**Fig. 5.7A**). All of the combination treated mice had no disease progression, indicating a complete or partial response or stable disease (**Fig. 5.7B**). Interestingly, over 70% of mice receiving erlotinib and dasatinib showed regression (**Fig. 5.7C**). At the end of treatment, mice were monitored for overall survival time. The combination group survived a median of 8.2 weeks from the beginning of treatment, showing an increase of approximately 2 weeks over the erlotinib alone group and an increase of approximately 3 weeks over the dasatinib alone group (**Fig. 5.7D**). To ensure that the combination of two drugs was not too toxic for the mice, thus preventing them from drinking the water containing doxycycline that drives transgene expression, their weight was monitored. No significant weight loss was seen in any of the treatment groups during treatment (**Fig. 5.7E**). The combination of erlotinib and dasatinib appears to have synergistic effects *in vivo*, improving outcomes in the CET mice.



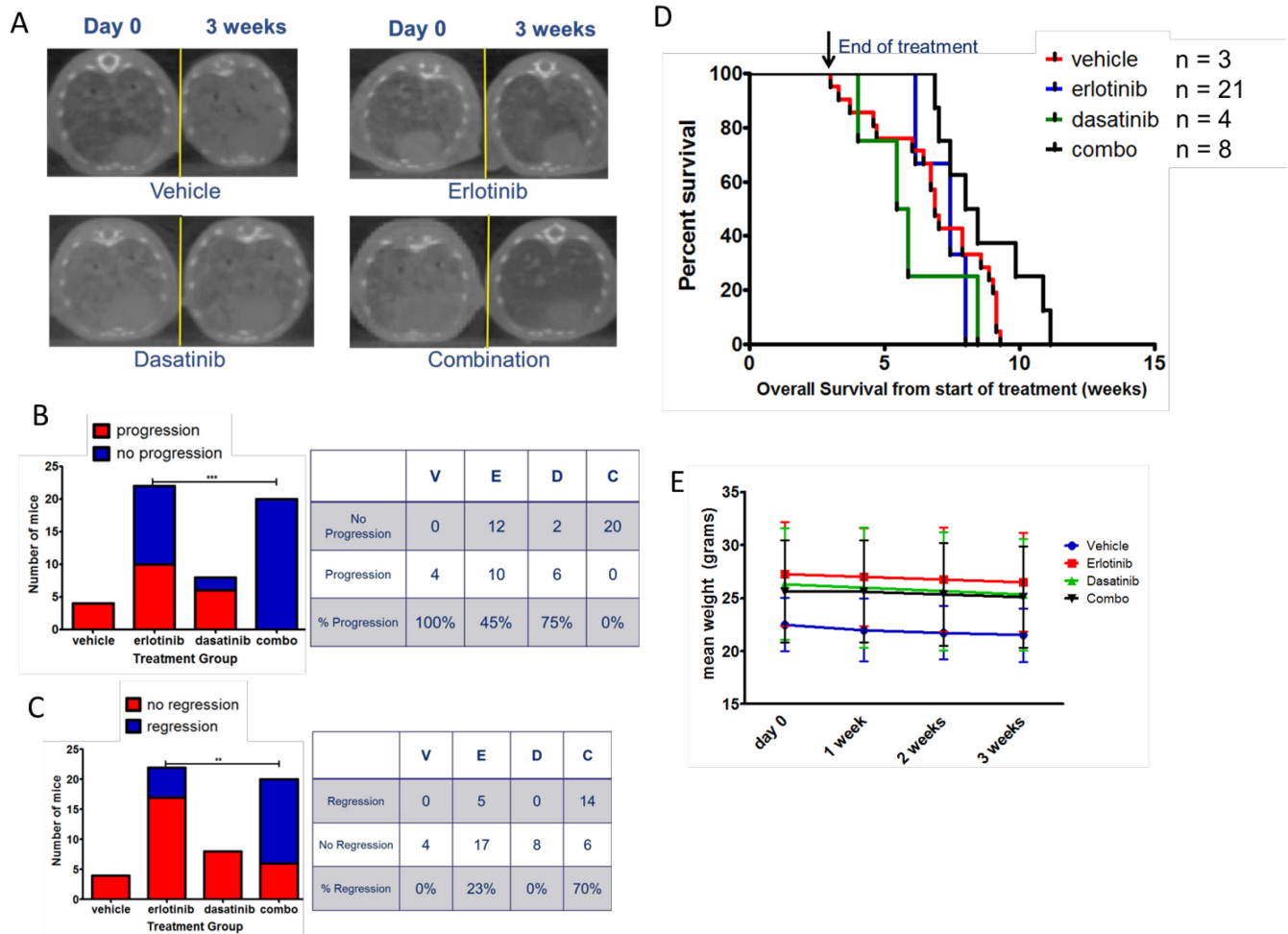


**Figure 5.7. Combination treatment with erlotinib and dasatinib overcomes resistance resulting from Twist1 expression.** (A) CT images from baseline and after 3 weeks of treatment for CET mice receiving vehicle, erlotinib alone, dasatinib alone or combination of erlotinib and dasatinib. CET mice receiving combination treatment show a decrease in tumor burden at the end of treatment compared to day 0. Other treatment groups show a drastic increase in tumor burden, or stable disease, despite 3 weeks of treatment. (B) Tumor burden, as visualized by CT image, was graded as before and no progression defined previously. No mice treated with the combination of erlotinib and dasatinib progressed. (C) Regression was a decrease in tumor burden grade at 3 weeks compared to baseline. Over 70% of combination treated CET mice regressed, while only about one fifth of erlotinib treated mice showed regression. Other treatment groups, vehicle and dasatinib alone, showed no regression (D) Kaplan-Meier overall survival from beginning of treatment. Median survival for CET combination mice was 8.2 weeks, for erlotinib treated mice was 6.8 weeks, for dasatinib treated mice was 5.6 weeks and vehicle was 7.4 weeks. (E) Mean weight of CET mice over the course of treatment, demonstrating minimal toxicity of combination treatment.

## **Bioinformatic Analysis of Erlotinib Resistance**

An unbiased gene expression approach to investigating potential resistance mechanisms was employed to complement the antibody array, which looked at changes in expression of a set of predefined proteins. RNA was isolated from the lung tissue of CE and CET mice that had been treated with vehicle or erlotinib for one week and microarray analysis was performed. The one week time point was the same used for the antibody array thus ideally allowing for comparison between microarray and antibody array results/hits. The microarray analysis allowed for a variety of comparisons to attempt to identify changes on the transcript level that could account for erlotinib resistance. Two different types of analyses were performed, Gene Set Enrichment Analysis (GSEA) and Ingenuity Pathway Analysis (IPA). One of the comparisons performed was interaction, which looked at genes expressed only as result of Twist1 overexpression and erlotinib treatment. The top significant gene sets from that interaction comparison are listed in table 5.1 and the top 15 of 25 significant genes (p value < 0.05) are listed in table 5.2. None of the top genes/gene sets directly supported the Src resistance mechanism.

An alternative analysis using IPA allowed for additional insight into gene expression differences between the genotypes and treatment groups. IPA provides particular molecules that are up or down regulated and associated networks, diseases and biological functions. This type of analysis focuses on changes in pathways, instead of particular genes or gene sets. Interestingly, several of the top networks from IPA involved aspects of the immune system, such as immune cell trafficking (**Fig. 5.8A**). Other networks that showed up as top hits were expected, including cell death and

survival and cellular growth and proliferation. Given some of the data demonstrating that overexpression of Twist1 decreases apoptosis in the presence of erlotinib, the cell death network was of particular interest. Networks involving particular molecules, such as Src, AKT, etc, can be mapped, resulting in a network map showing which associated molecules are up (red) or down regulated (green). This is a good visual representation of what is occurring throughout a signaling pathway of interest. In the interaction comparison, one of the significant networks was centered around AKT/MYC. Both the EGF ligand and amphiregulin were upregulated, which was an interesting result (**Fig. 5.8B**). These analyses did not directly implicate the Src pathway, but do not rule out its potential role in Twist1-mediated erlotinib resistance. Pathway analyses do point to the potential complexity of this resistance, and the many factors that may play a role in the shift from sensitive to resistant disease.

TOP SIGNIFICANT GENE SETS
VECCHI_GASTRIC_CANCER_ADVANCED_VS_EARLY_UP
SENESE_HDAC1_AND_HDAC2_TARGETS_DN
SENESE_HDAC2_TARGETS_DN
COLIN_PILOCYTIC_ASTROCYTOMA_VS_GLIOMASTOMA_DN
YAMASHITA_METHYLATED_IN_PROSTATE_CANCER
RUTELLA_RESPONSE_TO_CSF2RB_AND_IL4_UP
RUTELLA_RESPONSE_TO_HGF_UP
SWEET_LUNG_CANCER_KRAS_UP
MCLACHLAN_DENTAL_CARIES_DN
MCLACHLAN_DENTAL_CARIES_UP

**Table 5.1. Top significant gene sets.** The significant gene sets from the interaction comparison of microarray data for CE and CET mice treated with vehicle or erlotinib.

TOP SIGNIFICANT GENES	
Gene Symbol	Adj. P value
Tprn	0.005456
Kcne2	0.005456
Chil3	0.007948
Gpnmb	0.007948
Ctsk	0.007948
Spp1	0.010044
Corin	0.010044
NA	0.017868
H2-K1	0.017868
Uap1	0.028188
Phgr1	0.028188
Sec14l3	0.028188
H2-T23	0.028188
Auts2	0.028188
H2-T23	0.029068

**Table 5.2. Top significant genes.** Top 15 significant genes from interaction microarray comparison of CE and CET mice treated with vehicle or erlotinib.

A

**Top Networks**

ID	Associated Network Functions	Score
1	Cell Death and Survival, Cellular Compromise, Connective Tissue Disorders	30
2	Hematological System Development and Function, Immune Cell Trafficking, Inflammatory Response	24
3	Cell-To-Cell Signaling and Interaction, Hematological System Development and Function, Immune Cell Trafficking	16
4	Developmental Disorder, Cellular Development, Cellular Growth and Proliferation	2

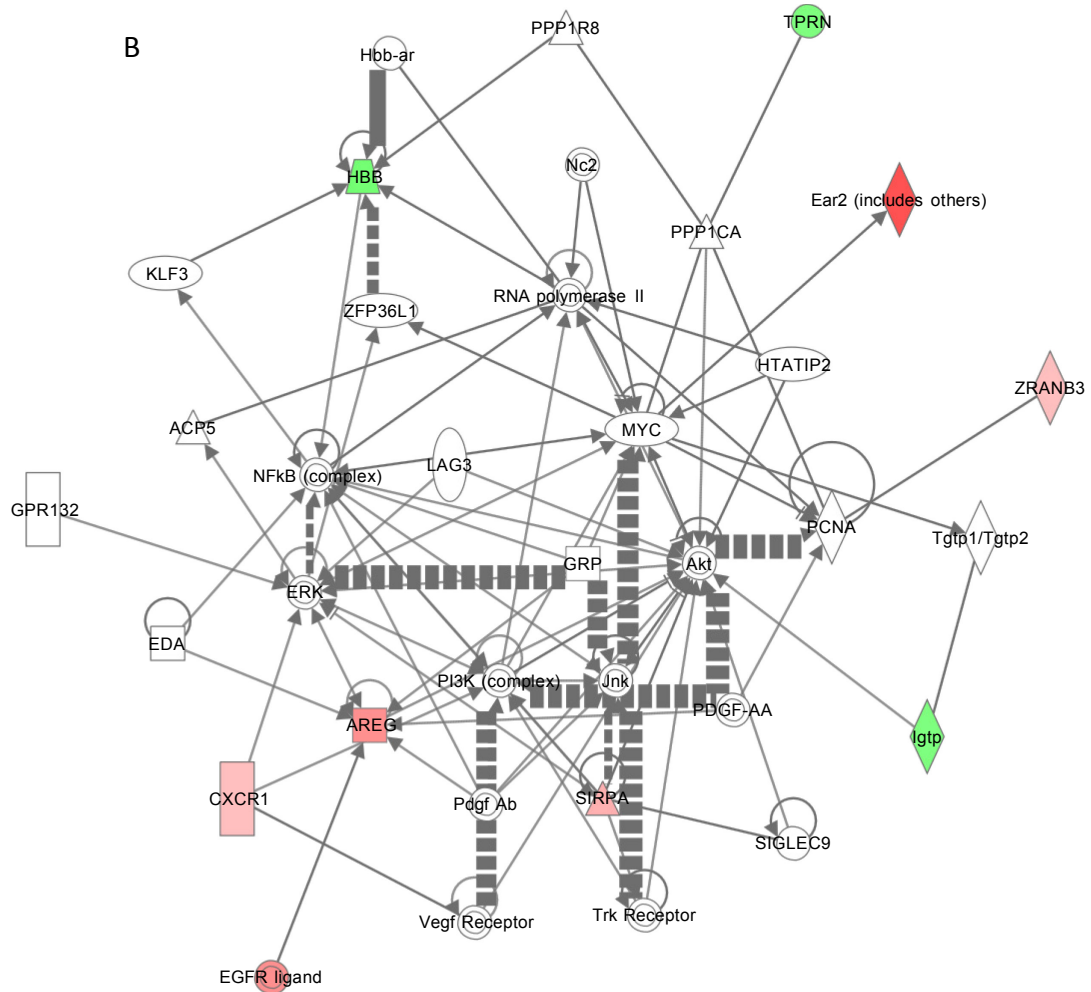


**Figure 5.8. Ingenuity Pathway Analysis.** (A) Top networks from IPA based off the interaction comparison. (B) MYC/AKT network from IPA showing up regulation (red) and down regulation (green) of molecules associated with the pathway and the interactions between the molecules.

## Section 5.2: Discussion

These results demonstrate that overexpression of Twist1, in the context of *EGFR* mutant NSCLC, leads to erlotinib resistance and through combination of erlotinib with a Src inhibitor, dasatinib, some of this resistance can be overcome. Having seen only minimal differences in tumor histology in CET versus CE mice, the effect of Twist1 on both tumor response and overall survival when mice were treated with erlotinib was surprising. While it might have been expected that a greater number of CET mice would have demonstrated resistance, in the context of progression/regression, the expression of Twist1 may have different effects in different mice, just as each individual patient's cancer is unique. Our data do clearly support the original hypothesis that Twist1 expression could result in increased erlotinib resistance.

Similar to what was seen in untreated animals, the levels of epithelial and mesenchymal markers does not qualitatively change, however further characterization may reveal subtle differences. The decrease in apoptosis seen in CET mice with erlotinib treatment, as indicated by levels of cleaved caspase 3, is interesting and indicates a potential role for Twist1 in regulation of apoptosis. Recent data has identified BIM as a target gene of TWIST1 and demonstrated that loss of BIM is sufficient to prevent apoptosis after TWIST1 inhibition (Yochum and Burns, personal communication). Upregulation of BIM is consistently seen with TKI-induced apoptosis and the loss of BIM is a known resistance mechanism to EGFR TKIs (73). Thus investigating the changes in levels of BIM in the CE and CET mice, with single and combination therapy, could reveal a mechanism of how TWIST1 is mediating erlotinib resistance.

Use of the antibody array was extremely helpful in identifying potential leads for the mechanism of resistance. While certain RTKs were expected to have altered phosphorylation levels, such as EGFR and perhaps Ax1, the appearance of a difference in phosphorylated Src was unexpected and exciting. This finding was supported by other studies published around the same time as well as some previous work that connected Src and TWIST1 (66-68), however a mechanism and the clinical implications are still undetermined. The bioinformatics data provided a wide variety of information that still needs to be analyzed to potentially help understand how Twist1 expression can lead to erlotinib resistance, both by Src-dependent and –independent mechanisms.

Clinical trials have been conducted, combining erlotinib and dasatinib, and the results have ultimately not supported the use of the combination patients with acquired resistance to erlotinib. Additionally, significant toxicities were observed with the combination (74). Conversely, in this study there was a clear reduction in tumor burden visible with the combination of erlotinib and dasatinib after only 5 days of treatment. This effect is amplified with longer treatment, leading to tumor regression in a majority of cases and prolonged overall survival. There appeared to be minimal toxicity to the mice from the combination of drugs.

A possibility is that Twist1 is acting independently of EMT, or multiple resistance mechanisms are arising as a result of Twist1 expression. All CET mice still do not respond to individual or combination treatment the same, as indicated by the different responses seen by CT scan and histologically. Further characterization is essential to explore the differences both between treatment groups and within a treatment group, as well as determining the effect of combination treatment in the CE mice. Identifying



markers that predict a response to the combination treatment would improve the design of clinical trials on combination therapies and ultimately treatment for NSCLC and patients facing acquired resistance.

### **Section 5.3: Conclusions**

Expression of Twist1 induces resistance to erlotinib in *EGFR* mutant NSCLC. As a result of Twist1 expression and erlotinib treatment, the levels of Src phosphorylation increases, indicating activation of Src. Combining erlotinib treatment with the Src inhibitor, dasatinib, in the CET mice leads to tumor regression, prolonged overall survival, as well as decreases in proliferation and downstream signaling. This indicates that the combined treatment overcomes the effect of Twist1 and resistance, resulting in a phenotype very similar to CE mice treated with erlotinib alone.

## **Chapter 6: Identification and Characterization of a novel TWIST1 inhibitor**

### **Section 6.1: Introduction**

Lung cancer is the leading cause of cancer death in the United States and worldwide. In 2015 alone, an estimated 221,200 new cases will be diagnosed and 158,040 lung cancer deaths will occur in the US (1). Recent advances in the treatment of NSCLC have come from recognition that NSCLC is not a single disease entity but rather a collection of distinct molecularly driven neoplasms. This paradigm is typified by the recent progress made in the treatment of patients with EGFR mutant and EML4-ALK translocation driven adenocarcinomas of the lung with tyrosine kinase inhibitors targeting these oncogenes (75). Unfortunately, little progress has been made in the treatment of patients with the most frequently observed driver oncogene, mutant KRAS. KRAS is mutated in one third of all malignancies and approximately 25% of all NSCLC (76). Furthermore, acquired resistance to the currently targetable driver mutations is all but inevitable (77, 78). New strategies are needed to effectively and durably target oncogene driven NSCLC.

Oncogene induced senescence (OIS) is an irreversible cell cycle arrest that is characterized by cells displaying an enlarged, flattened cytoplasm, increased senescence associated beta-galactosidase (SA- $\beta$ -Gal) activity, increased chromatin condensation and changes in gene expression associated with DNA damage and cell cycle checkpoint pathways. OIS is thought to be triggered early during tumorigenesis after oncogene activation and serves as a checkpoint to prevent pre-malignant lesions from progressing to malignancy (79). The bypass of senescence in mouse models of Kras-mediated adenocarcinoma of the lung and pancreas is essential for tumorigenesis (62, 80, 81). We

have shown that TWIST1 is required for suppression of OIS (39, 82). Pro-senescence therapy in oncogene driven NSCLC through inhibition of key downstream mediators that suppress OIS would be a valuable treatment.

Apoptosis is a cellular process that leads to activation of “executioner” cysteine aspartate- specific proteases (caspases), which cleave a variety of cellular substrates leading to cell death (83). Apoptosis eliminates cells in response to a number of cellular stresses, including genome instability, oncogene activation, or hypoxia (83). We have demonstrated that TWIST1 is required to suppress apoptosis in a subset of oncogene driven NSCLC (39). Cancer cells frequently evade apoptosis and therefore, reactivation of suppressed apoptotic pathways in NSCLC would be a valuable therapeutic strategy.

TWIST1 is a basic helix-loop-helix (bHLH) transcription factor that plays critical roles at multiple stages of organismal development (84). A number of reports have implicated TWIST1 in oncogenesis through its ability to inhibit apoptosis, prevent OIS and promote metastasis through induction of the epithelial-mesenchymal transition (EMT) (37, 47, 85-89). Increased TWIST1 expression is also correlated with increased risk of metastasis and poor prognosis in a number of solid tumor types including lung (90). We have demonstrated that Twist1 cooperates with mutant Kras to induce lung adenocarcinoma in vivo and that inhibition of Twist1 in vivo and in human lung cancer cell lines led to OIS and in some cases, apoptosis (39, 82). Furthermore, we have found that TWIST1 is essential for tumor maintenance in human NSCLC characterized by defined oncogenic drivers including *KRAS* mutant, *EGFR* mutant and *MET* amplified/mutant tumors (39). Interestingly, the *KRAS*, *EGFR* and *MET* oncogenes activate common downstream signaling pathways including the RAF/MAPK and

PI3K/AKT pathways. Furthermore, the reciprocal crosstalk between EGFR and MET is well established and has significant therapeutic implications (91). Studying the role of TWIST1-E2A pathway in these three interrelated driver mutations could potentially lead to the development of therapies for patients bearing these driver mutations.

TWIST1 functions as both a homo- and heterodimeric transcription factor and its choice of transcriptional binding partner can greatly influence its ability to modulate transcriptional activity and function (92). E12 and E47 are two transcription factors encoded through alternative splicing by the E2A locus that differ only in their bHLH domain. They can act either as tumor suppressors through inhibition of cell proliferation and promotion of apoptosis as seen in several lymphoid malignancies (93), or can function as oncogenes in solid tumors such as prostate cancer (94) and possibly in breast cancer (95). TWIST1 forms functional heterodimers with either E12 or E47 during limb development and cranial fusion (84). Furthermore studies in osteoblasts have shown that TWIST1 heterodimerization with E12 can stabilize TWIST1 by preventing its lysosomal degradation (96). The role of the TWIST1-E12/E47 heterodimer in cancer is unknown; however, our preliminary data suggests that the E2A protein play a key role in mediating TWIST1 dependent tumorigenesis.

Having identified TWIST1 as a prospective target, we employed a combined bioinformatic-chemical approach to identify pharmacologic inhibitors of TWIST1 using a CMAP analysis (**Fig. 6.1**) (97). We used gene expression profiles from several KRAS mutant human lung cancer cell lines following shRNA-mediated TWIST1 knockdown to perform a CMap analysis (**Fig 6.1**), in an attempt to identify candidate agents that targeted TWIST1. We identified and demonstrated that the harmala alkaloid, harmine

phenocopied the growth inhibition observed with silencing of TWIST1 by inducing OIS or apoptosis in oncogene driver defined NSCLC cell lines (**Fig 6.2A** and data not shown). Remarkably, these effects were associated with a decrease in TWIST1 levels through protein degradation in vitro (**Fig. 6.2B & C**). This demonstrates potential for harmine as a pharmacologic inhibitor of TWIST1.

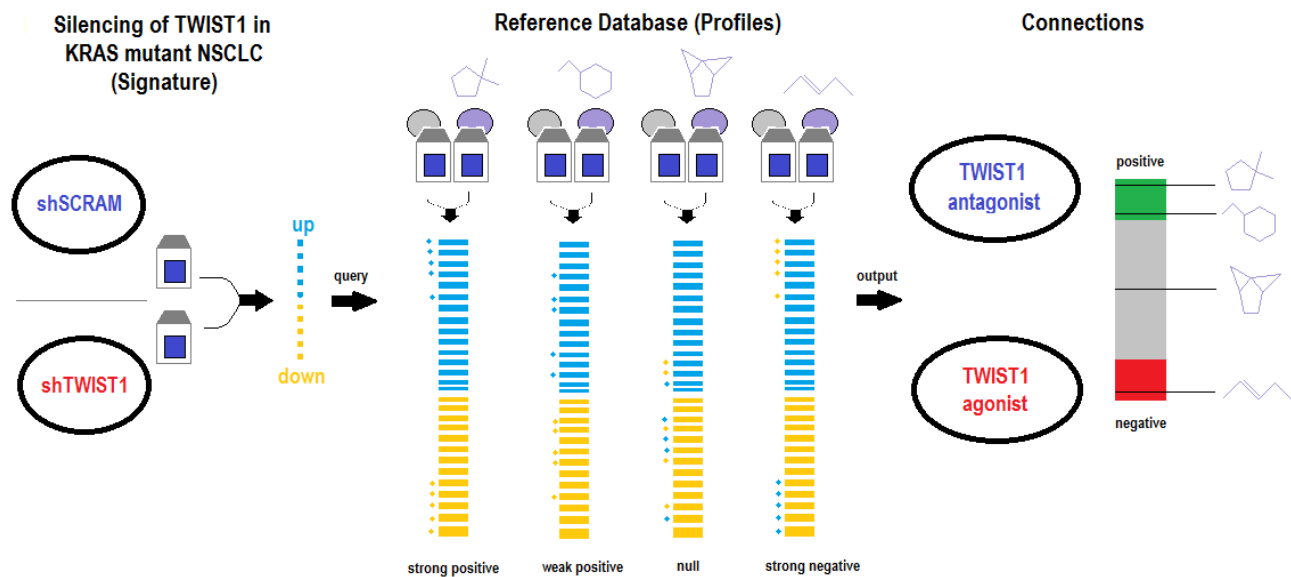


**Figure 5.1. Overview of CMap Analysis.** Microarray data from knockdown of TWIST1 in human *KRAS* mutant NSCLC cell lines is fed into the CMap database and the gene signature compared to those produced by all the drugs, genetic agents, etc in the database. The output provides compounds that have a gene signature similar to or opposite of knockdown of TWIST1. This does not necessarily mean that the drug targets TWIST1.

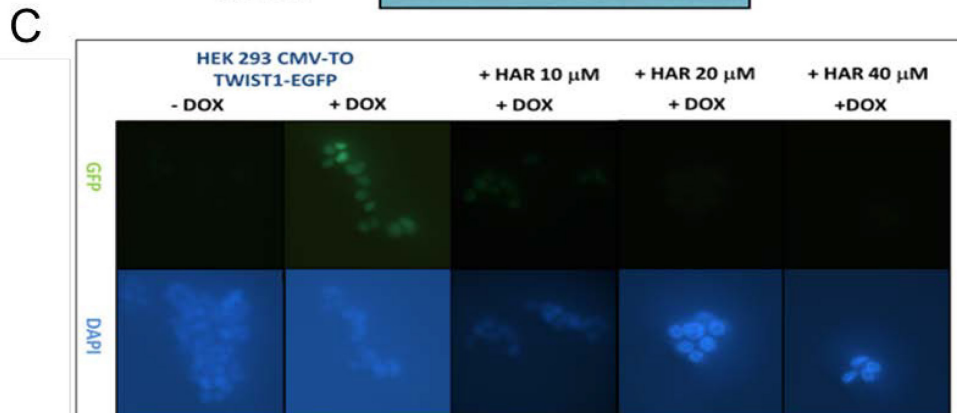
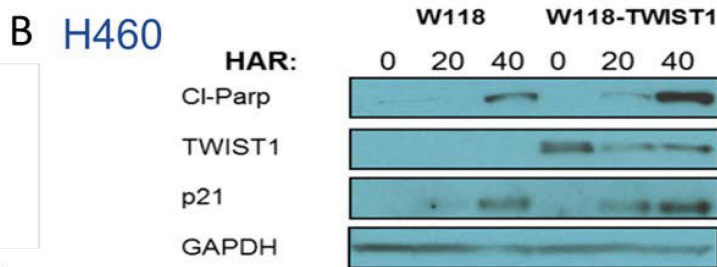
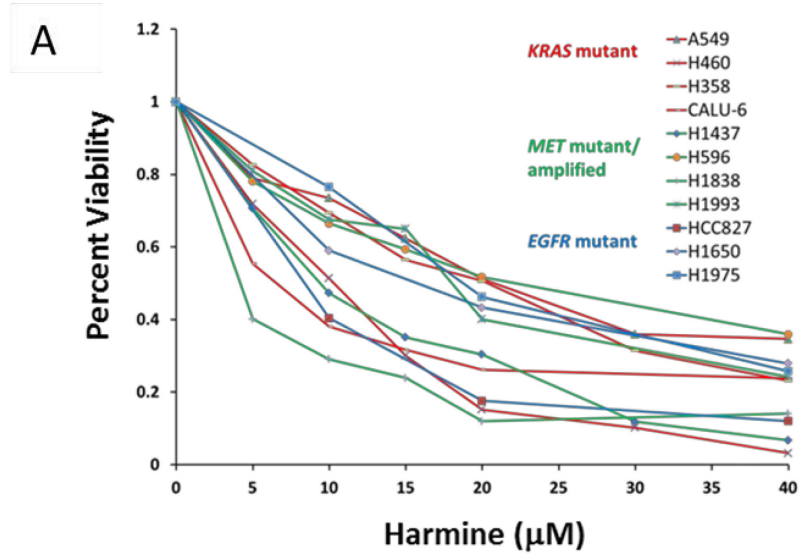


**Figure 6.2. . Harmine inhibits growth through degradation of TWIST1 in oncogene driver define NSCLC cell lines.** Harmine, identified through connectivity mapping (CMAP) demonstrates through (A) MTS assay growth inhibition in the indicated NSCLC cells in a dose and time dependent manner (B) Western blot demonstrating reduction of exogenous TWIST1 protein expression as well as induction of p21 after 72 hrs of harmine treatment. (C) Fluorescence microscopy (20X) demonstrating nuclear localization of TWIST1-EGFP (green). DAPI stain (blue) was used to stain the nucleus after addition of 500 ng/ml doxycycline and subsequent decrease in TWIST1 expression after co-treatment with increasing doses of harmine. (unpublished data).

## **Section 6.2: Materials and Methods**

### **Immunoblot analysis**

Homogenized lung tissue were lysed on ice for 60 minutes in radioimmunoprecipitation assay buffer supplemented with protease and phosphatase inhibitors (Sigma-Aldrich) and clarified by centrifugation. Protein concentrations were determined by Pierce Micro BCA protein assay (Thermo Fisher Scientific). Equal protein concentrations of each sample were run on NuPAGE bis-Tris gels (Invitrogen) and electrophoretically transferred to polyvinylidene difluoride membranes. After being blocked with 5% dried milk in TBS containing 0.2% Tween 20, the filters were incubated with primary antibodies. The following primary antibodies were used: anti-cleaved Parp (9548, Cell Signaling), anti-Twist1 (sc-81417, Santa Cruz), anti-GAPDH (FL-335, Santa Cruz), and anti-luciferase (20R-1419, Fitzgerald). After washing and incubation with horseradish peroxidase (HRP)-conjugated anti-rabbit or anti-mouse IgG (Amersham, Piscataway, NJ), the antigen-antibody complexes were visualized by chemiluminescence (ECL detection system; Perkin Elmer, Boston, MA).

### **Histology and immunohistochemistry**

Tissues were fixed in 10% buffered formalin for 24 h and then transferred to 70% ethanol until embedding in paraffin. Tissue sections 5  $\mu$ m thick were cut from paraffin embedded blocks, placed on glass slides and hematoxylin and eosin (H&E) staining was performed using standard procedures (Johns Hopkins Histology Core). Antibodies used in our study: Ki-67 (Leica Biosystems) and cleaved caspase 3 (Cell Signaling). Samples were dewaxed in xylene and rehydrated in a graded series of ethanols. Antigen retrieval was performed by 45 min rice-cooker irradiation in citrate-based Antigen Unmasking



Solution (Vector Laboratories, Burlingame, CA, USA). Endogenous peroxidases were blocked in 3% hydrogen peroxide in methanol for 10 minutes. Non-specific binding was blocked with 2% bovine serum for 60 minutes. Primary antibodies were used at appropriate dilutions (Ki-67 at 1:2000 and cleaved caspase 3 at 1:500) and sections incubated overnight at 4 degrees Celsius. Secondary incubation was done using PowerVision Poly-HRP anti-rabbit IgG (Leica Biosystems). Visualization was performed using DAB substrate kit for Peroxidase (Vector Laboratories). Sections were counterstained with Gill's hematoxylin (Vector Laboratories) and slides were mounted in aqueous mounting media (Vector Laboratories).

### **Transgenic mice**

Mice were housed in groups of no more than five per cage with free access to food and water, under controlled light/dark cycles, in facilities with regulated temperature and humidity. Mice were randomly assigned to different experimental groups. All procedures were approved by the Institutional Animal Care and Use Committee of The Johns Hopkins University.

Inducible Twist1/Kras<sup>G12D</sup> transgenic mice in the FVB/N inbred background were of the genotype: CCSP-rtTA/tetO-Kras<sup>G12D</sup>/Twist1-tetO-luc (CRT). All the mice were weaned 3–4 weeks of age and then placed on dox at 4–8 weeks of age. The mice treated had similar levels of tumor burden per CT.

Harmine was purchased from Sigma Aldrich (St. Louis, MO). For in vivo experiments, harmine was dissolved in normal saline by heating and sonication. The mice

received 10 mg/kg harmine or normal saline via intraperitoneal injection daily, 5 days a week for 3 weeks.

### Section 6.3: Results

Having the preliminary data demonstrate the effect of harmine on *KRAS* mutant NSCLC cell lines, we wanted to determine what effect, if any, the drug would have on an *in vivo* model of lung adenocarcinoma. We treated the CCSP-rtTA/tetO-*Kras*<sup>G12D</sup>/*Twist1*-tetO7-luc (CRT) mice (39) with harmine for 3 weeks and measured the lung tumor volume in each mouse at baseline and weekly with serial microCT. Micro-computed tomography (mCT) images, comparing tumor volume and baseline and at the end of treatment, revealed that treatment with harmine decreases the tumor volume growth rate (**Fig. 6.3**). Treatment of the animals with harmine had no observable toxicity on the animals and body weight was unaffected by harmine treatment suggesting that the doses used were safe and efficacious.

We then examined the potential mechanisms of growth inhibition after harmine treatment. We first examined whether a decrease in proliferation was responsible for the observed growth inhibition, however, we observed no significant difference in proliferation rate as measured by Ki-67 staining (**Fig. 6.4**). We next examined whether increased apoptosis contributed to the growth inhibitory effects of harmine. Remarkably, we observed increased apoptosis with harmine as measured by cleaved caspase 3 staining (**Fig. 6.4**) and cleaved PARP (**Fig. 6.5**). Furthermore, harmine treatment leads to marked decrease in *Twist1* in the lung tumors (**Fig. 6.5**). Thus harmine has cytotoxic effects *in vivo* on *Kras* mutant, *Twist1* overexpressing lung adenocarcinoma which are accompanied by *Twist1* degradation.

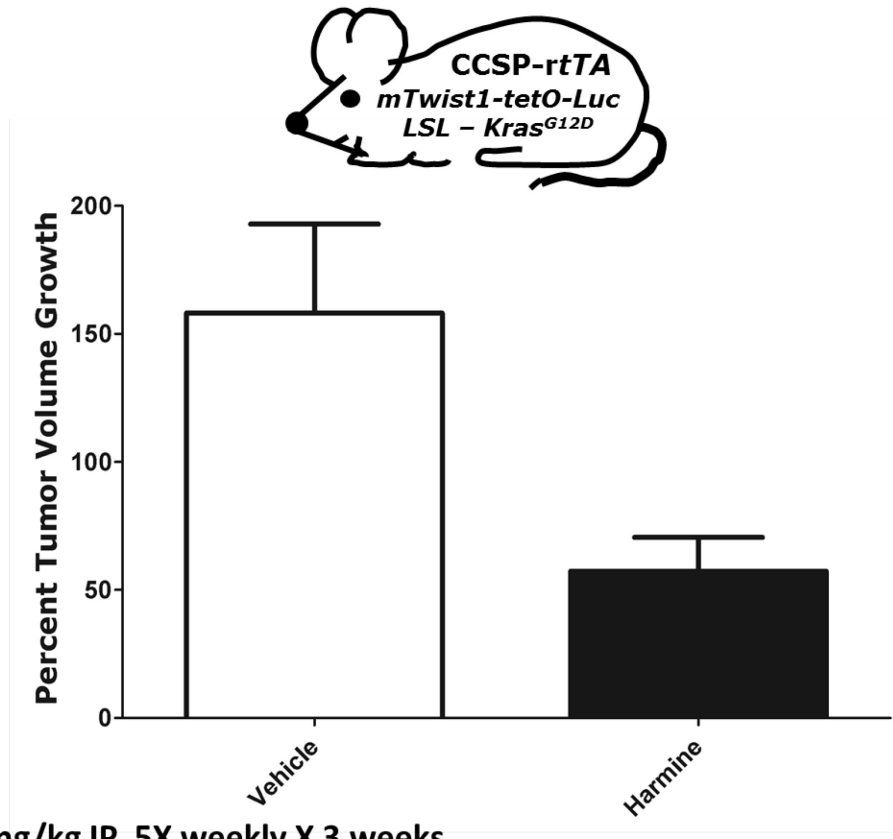


**Figure 6.3. Harmine has activity in a Kras<sup>G12D</sup>/Twist1 murine model of lung adenocarcinoma.** Lung tumor growth rate is decreased after 3 weeks of treatment with harmine in the CCSP-rtTA/tetO-*Kras<sup>G12D</sup>/Twist1-tetO7-luc* (CRT) mice. Lung tumor volume was measured at baseline and weekly with serial CT in the same CRT mouse. Micro-computed tomography (mCT) images were reviewed by a board certified radiation oncologist on multiple index tumors in a blinded fashion (n= 2–5 tumors per mouse). Volumes were normalized to the starting volume, t= 0 before harmine treatment, and percent tumor volume growth was then calculated by (normalized tumor vol. X 100%) - 100%.

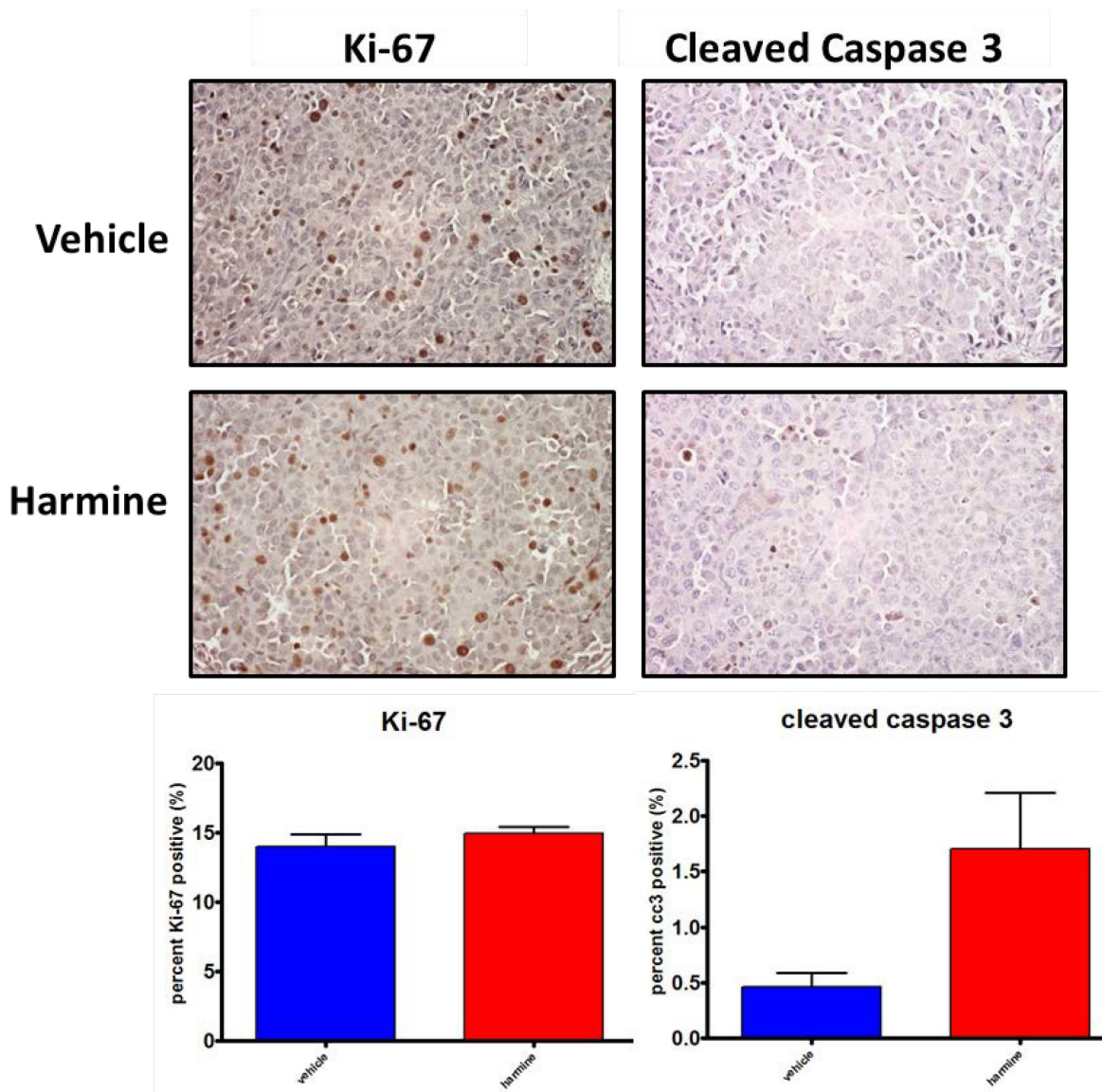


**Figure 6.4. Harmine treatment alters some cellular processes in a KrasG12D/Twist1 murine model of lung adenocarcinoma.** Treatment with harmine results in similar proliferation levels as measured by Ki-67 staining (UPPER LEFT) and increased apoptosis (UPPER RIGHT) as measured by cleaved caspase 3 staining indicated by black arrows. LOWER: Quantification of Ki-67 staining ( $p=0.3621$ ) and Cleaved caspase 3 IHC ( $p=0.0453$ ).

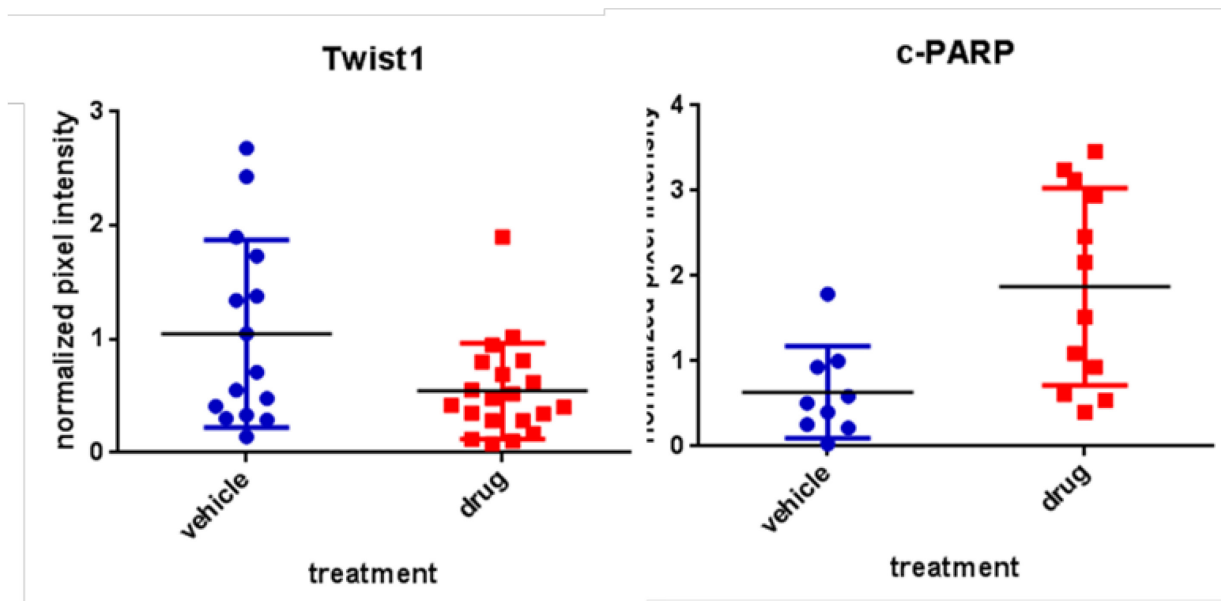


**Figure 6.5. Harmine decreases Twist1 levels in a *Kras*<sup>G12D</sup>/*Twist1* murine model of lung adenocarcinoma.** Quantitation of Twist1 and cleaved PARP protein levels in vehicle and harmine treated animals at 3 weeks. Proteins were normalized to luciferase protein levels to control for possible differences in tumor burden. Differences were statistically significant for Twist1,  $P < 0.04$  and c-PARP,  $P < 0.005$  respectively.

## Section 6.4: Discussion and Conclusions

This study demonstrates the ability of harmine to target Twist1 and slow tumor growth in the CRT mouse model. Targeting mutant *KRAS* has been largely unsuccessful (76) and another potential cancer therapy target, transcription factors, are difficult to inhibit pharmacologically (98). However through use of Connectivity Mapping bioinformatics analysis, the potential Twist1 inhibitor, harmine, was identified. Preliminary *in vitro* data demonstrated Twist1 inhibition and this was confirmed *in vivo*. The levels of Twist1 decreased in harmine treated mice, however whether the drug was targeting Twist1, or one of its binding partners, which then led to Twist1 degradation was not clearly demonstrated. Preliminary data suggests this is through disruption of the TWIST1-E12/E47 heterodimer. Further experimentation is required to determine the actual target of harmine *in vivo*. Harmine is known to inhibit DYRK kinases and it is possible that some of the growth inhibitory effects are TWIST1 independent. The observed *in vitro* growth inhibitory effects are at least partially dependent on the TWIST1-E2A pathway, as overexpression of either TWIST1, E12, E47, TWIST1-E12 or TWIST1-E47, but not TWIST1-TWIST1 can rescue harmine induced growth inhibition.

While tumor regression was not seen, the slowing of tumor growth can still be considered an improvement in the treatment of *KRAS* mutant lung cancer. The increase in levels of cleaved caspase 3 and cleaved PARP with harmine treatment could indicate the involvement of Twist1 in regulation of apoptosis. Twist1 may inhibit apoptosis, allowing for tumor growth; decreased levels of Twist1 as a result of harmine treatment allows for the increase in apoptosis resulting in the slowing of tumor growth. Future experiments,

both *in vitro* and *in vivo*, can look at how Twist1 regulates apoptosis in the context of mutant *KRAS* lung cancer.

Harmine and related compounds were identified through CMap, however drug screening could be performed in an attempt to find a more potent and less neurotoxic derivative of harmine or another inhibitor altogether. In addition, as harmine treatment affects TWIST1 levels, the combination of harmine and erlotinib could be studied in the context of *EGFR* mutant NSCLC. Similar to the experiments combining erlotinib and dasatinib in the CE and CET mice, treating the mice with harmine could help identify the mechanism of how TWIST1 is leading to erlotinib resistance.

## Chapter 7: References

1. Siegel RL, Miller KD, Jemal A. Cancer statistics, 2015. *CA: a cancer journal for clinicians*. 2015;65(1):5-29.
2. Ettinger DS, Wood DE, Akerley W, Bazhenova LA, Borghaei H, Camidge DR, et al. Non-Small Cell Lung Cancer, Version 6.2015. *Journal of the National Comprehensive Cancer Network : JNCCN*. 2015;13(5):515-24.
3. Garraway LA, Janne PA. Circumventing cancer drug resistance in the era of personalized medicine. *Cancer discovery*. 2012;2(3):214-26.
4. Camidge DR, Pao W, Sequist LV. Acquired resistance to TKIs in solid tumours: learning from lung cancer. *Nature reviews Clinical oncology*. 2014;11(8):473-81.
5. Sharma SV, Settleman J. Oncogene addiction: setting the stage for molecularly targeted cancer therapy. *Genes & development*. 2007;21(24):3214-31.
6. Faber AC, Li D, Song Y, Liang MC, Yeap BY, Bronson RT, et al. Differential induction of apoptosis in HER2 and EGFR addicted cancers following PI3K inhibition. *Proceedings of the National Academy of Sciences of the United States of America*. 2009;106(46):19503-8. PMID: 2765921.
7. Arora A, Scholar EM. Role of tyrosine kinase inhibitors in cancer therapy. *The Journal of pharmacology and experimental therapeutics*. 2005;315(3):971-9.
8. Hidalgo M, Bloedow D. Pharmacokinetics and pharmacodynamics: maximizing the clinical potential of Erlotinib (Tarceva). *Seminars in oncology*. 2003;30(3 Suppl 7):25-33.
9. Paez JG, Janne PA, Lee JC, Tracy S, Greulich H, Gabriel S, et al. EGFR mutations in lung cancer: correlation with clinical response to gefitinib therapy. *Science*. 2004;304(5676):1497-500.
10. Lynch TJ, Bell DW, Sordella R, Gurubhagavatula S, Okimoto RA, Brannigan BW, et al. Activating mutations in the epidermal growth factor receptor underlying responsiveness of non-small-cell lung cancer to gefitinib. *The New England journal of medicine*. 2004;350(21):2129-39.
11. Pao W, Miller V, Zakowski M, Doherty J, Politi K, Sarkaria I, et al. EGF receptor gene mutations are common in lung cancers from "never smokers" and are associated with sensitivity of tumors to gefitinib and erlotinib. *Proceedings of the National Academy of Sciences of the United States of America*. 2004;101(36):13306-11. PMID: 516528.
12. Sequist LV, Waltman BA, Dias-Santagata D, Digumarthy S, Turke AB, Fidias P, et al. Genotypic and histological evolution of lung cancers acquiring resistance to EGFR inhibitors. *Science translational medicine*. 2011;3(75):75ra26. PMID: 3132801.
13. Ettinger DS, Bepler G, Bueno R, Chang A, Chang JY, Chirieac LR, et al. Non-



small cell lung cancer clinical practice guidelines in oncology. *Journal of the National Comprehensive Cancer Network : JNCCN*. 2006;4(6):548-82.

14. Irmer D, Funk JO, Blaukat A. EGFR kinase domain mutations - functional impact and relevance for lung cancer therapy. *Oncogene*. 2007;26(39):5693-701.
15. Pao W, Miller VA, Politi KA, Riely GJ, Somwar R, Zakowski MF, et al. Acquired Resistance of Lung Adenocarcinomas to Gefitinib or Erlotinib Is Associated with a Second Mutation in the EGFR Kinase Domain. *PLoS Med*. 2005;2(3):e73.
16. Bean J, Brennan C, Shih JY, Riely G, Viale A, Wang L, et al. MET amplification occurs with or without T790M mutations in EGFR mutant lung tumors with acquired resistance to gefitinib or erlotinib. *Proceedings of the National Academy of Sciences of the United States of America*. 2007;104(52):20932-7. PMID: 2409244.
17. Engelman JA, Zejnullahu K, Mitsudomi T, Song Y, Hyland C, Park JO, et al. MET amplification leads to gefitinib resistance in lung cancer by activating ERBB3 signaling. *Science*. 2007;316(5827):1039-43.
18. Sos ML, Koker M, Weir BA, Heynck S, Rabinovsky R, Zander T, et al. PTEN loss contributes to erlotinib resistance in EGFR-mutant lung cancer by activation of Akt and EGFR. *Cancer research*. 2009;69(8):3256-61. PMID: 2849653.
19. Takezawa K, Pirazzoli V, Arcila ME, Nebhan CA, Song X, de Stanchina E, et al. HER2 amplification: a potential mechanism of acquired resistance to EGFR inhibition in EGFR-mutant lung cancers that lack the second-site EGFR T790M mutation. *Cancer discovery*. 2012;2(10):922-33. PMID: 3473100.
20. Zhang Z, Lee JC, Lin L, Olivas V, Au V, LaFramboise T, et al. Activation of the AXL kinase causes resistance to EGFR-targeted therapy in lung cancer. *Nature genetics*. 2012;44(8):852-60. PMID: 3408577.
21. Suda K, Tomizawa K, Fujii M, Murakami H, Osada H, Maehara Y, et al. Epithelial to mesenchymal transition in an epidermal growth factor receptor-mutant lung cancer cell line with acquired resistance to erlotinib. *Journal of thoracic oncology : official publication of the International Association for the Study of Lung Cancer*. 2011;6(7):1152-61.
22. Buonato JM, Lazzara MJ. ERK1/2 blockade prevents epithelial-mesenchymal transition in lung cancer cells and promotes their sensitivity to EGFR inhibition. *Cancer research*. 2014;74(1):309-19. PMID: 3964587.
23. Stewart EL, Tan SZ, Liu G, Tsao MS. Known and putative mechanisms of resistance to EGFR targeted therapies in NSCLC patients with EGFR mutations-a review. *Translational lung cancer research*. 2015;4(1):67-81. PMID: 4367712.
24. Thomson S, Buck E, Petti F, Griffin G, Brown E, Ramnarine N, et al. Epithelial to

mesenchymal transition is a determinant of sensitivity of non-small-cell lung carcinoma cell lines and xenografts to epidermal growth factor receptor inhibition. *Cancer research*. 2005;65(20):9455-62.

25. Frederick BA, Helfrich BA, Coldren CD, Zheng D, Chan D, Bunn PA, Jr., et al. Epithelial to mesenchymal transition predicts gefitinib resistance in cell lines of head and neck squamous cell carcinoma and non-small cell lung carcinoma. *Molecular cancer therapeutics*. 2007;6(6):1683-91.

26. Fuchs BC, Fujii T, Dorfman JD, Goodwin JM, Zhu AX, Lanuti M, et al. Epithelial-to- mesenchymal transition and integrin-linked kinase mediate sensitivity to epidermal growth factor receptor inhibition in human hepatoma cells. *Cancer research*. 2008;68(7):2391-9.

27. Coldren CD, Helfrich BA, Witta SE, Sugita M, Lapadat R, Zeng C, et al. Baseline gene expression predicts sensitivity to gefitinib in non-small cell lung cancer cell lines. *Molecular cancer research : MCR*. 2006;4(8):521-8.

28. Rho JK, Choi YJ, Lee JK, Ryoo BY, Na, II, Yang SH, et al. Epithelial to mesenchymal transition derived from repeated exposure to gefitinib determines the sensitivity to EGFR inhibitors in A549, a non-small cell lung cancer cell line. *Lung cancer*. 2009;63(2):219-26.

29. Jackman D, Pao W, Riely GJ, Engelman JA, Kris MG, Janne PA, et al. Clinical definition of acquired resistance to epidermal growth factor receptor tyrosine kinase inhibitors in non-small-cell lung cancer. *Journal of clinical oncology : official journal of the American Society of Clinical Oncology*. 2010;28(2):357-60. PMID: 3870288.

30. Kalluri R, Weinberg RA. The basics of epithelial-mesenchymal transition. *The Journal of clinical investigation*. 2009;119(6):1420-8. PMID: 2689101.

31. Yang J, Weinberg RA. Epithelial-mesenchymal transition: at the crossroads of development and tumor metastasis. *Developmental cell*. 2008;14(6):818-29.

32. Acloque H, Thiery JP, Nieto MA. The physiology and pathology of the EMT. Meeting on the epithelial-mesenchymal transition. *EMBO reports*. 2008;9(4):322-6. PMID: 2288772.

33. Hay E. Elizabeth Hay interviewed by Fiona Watt. *Journal of cell science*. 2004;117(Pt 20):4617-8.

34. Thiery JP, Acloque H, Huang RY, Nieto MA. Epithelial-mesenchymal transitions in development and disease. *Cell*. 2009;139(5):871-90.

35. Peinado H, Olmeda D, Cano A. Snail, Zeb and bHLH factors in tumour progression: an alliance against the epithelial phenotype? *Nature reviews Cancer*. 2007;7(6):415-28.

36. Pallier K, Cessot A, Cote JF, Just PA, Cazes A, Fabre E, et al. TWIST1 a

new determinant of epithelial to mesenchymal transition in EGFR mutated lung adenocarcinoma. *PloS one*. 2012;7(1):e29954. PMID: 3260187.

37. Yang J, Mani SA, Donaher JL, Ramaswamy S, Itzykson RA, Come C, et al. Twist, a master regulator of morphogenesis, plays an essential role in tumor metastasis. *Cell*. 2004;117(7):927-39.

38. Vichalkovski A, Gresko E, Hess D, Restuccia DF, Hemmings BA. PKB/AKT phosphorylation of the transcription factor Twist-1 at Ser42 inhibits p53 activity in response to DNA damage. *Oncogene*. 2010;29(24):3554-65.

39. Tran PT, Shroff EH, Burns TF, Thiyagarajan S, Das ST, Zabuawala T, et al. Twist1 suppresses senescence programs and thereby accelerates and maintains mutant Kras- induced lung tumorigenesis. *PLoS genetics*. 2012;8(5):e1002650. PMID: 3360067.

40. Chen ZF, Behringer RR. twist is required in head mesenchyme for cranial neural tube morphogenesis. *Genes & development*. 1995;9(6):686-99.

41. Entz-Werle N, Stoetzel C, Berard-Marec P, Kalifa C, Brugiere L, Pacquement H, et al. Frequent genomic abnormalities at TWIST in human pediatric osteosarcomas. *International journal of cancer Journal international du cancer*. 2005;117(3):349-55.

42. Hoek K, Rimm DL, Williams KR, Zhao H, Ariyan S, Lin A, et al. Expression profiling reveals novel pathways in the transformation of melanocytes to melanomas. *Cancer research*. 2004;64(15):5270-82.

43. Kwok WK, Ling MT, Lee TW, Lau TC, Zhou C, Zhang X, et al. Up-regulation of TWIST in prostate cancer and its implication as a therapeutic target. *Cancer research*. 2005;65(12):5153-62.

44. Mironchik Y, Winnard PT, Jr., Vesuna F, Kato Y, Wildes F, Pathak AP, et al. Twist overexpression induces in vivo angiogenesis and correlates with chromosomal instability in breast cancer. *Cancer research*. 2005;65(23):10801-9.

45. Ohuchida K, Mizumoto K, Ohhashi S, Yamaguchi H, Konomi H, Nagai E, et al. Twist, a novel oncogene, is upregulated in pancreatic cancer: clinical implication of Twist expression in pancreatic juice. *International journal of cancer Journal international du cancer*. 2007;120(8):1634-40.

46. Zhang Z, Xie D, Li X, Wong YC, Xin D, Guan XY, et al. Significance of TWIST expression and its association with E-cadherin in bladder cancer. *Human pathology*. 2007;38(4):598-606.

47. Ansieau S, Morel AP, Hinkal G, Bastid J, Puisieux A. TWISTing an embryonic transcription factor into an oncoprotein. *Oncogene*. 2010;29(22):3173-84.

48. Cerami E, Gao J, Dogrusoz U, Gross BE, Sumer SO, Aksoy BA, et al. The cBio cancer genomics portal: an open platform for exploring multidimensional cancer genomics data. *Cancer discovery*. 2012;2(5):401-4. PMID: 3956037.
49. Gao J, Aksoy BA, Dogrusoz U, Dresdner G, Gross B, Sumer SO, et al. Integrative analysis of complex cancer genomics and clinical profiles using the cBioPortal. *Science signaling*. 2013;6(269):pl1. PMID: 4160307.
50. Zhang X, Wang Q, Ling MT, Wong YC, Leung SC, Wang X. Anti-apoptotic role of TWIST and its association with Akt pathway in mediating taxol resistance in nasopharyngeal carcinoma cells. *International journal of cancer Journal international du cancer*. 2007;120(9):1891-8.
51. Sharif MN, Sosic D, Rothlin CV, Kelly E, Lemke G, Olson EN, et al. Twist mediates suppression of inflammation by type I IFNs and Axl. *The Journal of experimental medicine*. 2006;203(8):1891-901. PMID: 2118370.
52. Moffat J, Grueneberg DA, Yang X, Kim SY, Kloepfer AM, Hinkle G, et al. A lentiviral RNAi library for human and mouse genes applied to an arrayed viral high-content screen. *Cell*. 2006;124(6):1283-98.
53. Zhou G, Wang S, Wang Z, Zhu X, Shu G, Liao W, et al. Global comparison of gene expression profiles between intramuscular and subcutaneous adipocytes of neonatal landrace pig using microarray. *Meat science*. 2010;86(2):440-50.
54. Carvalho BS, Irizarry RA. A framework for oligonucleotide microarray preprocessing. *Bioinformatics*. 2010;26(19):2363-7. PMID: 2944196.
55. Benjamini Y, Drai D, Elmer G, Kafkafi N, Golani I. Controlling the false discovery rate in behavior genetics research. *Behavioural brain research*. 2001;125(1-2):279-84.
56. Chmielecki J, Foo J, Oxnard GR, Hutchinson K, Ohashi K, Somwar R, et al. Optimization of dosing for EGFR-mutant non-small cell lung cancer with evolutionary cancer modeling. *Science translational medicine*. 2011;3(90):90ra59. PMID: 3500629.
57. Ohashi K, Sequist LV, Arcila ME, Moran T, Chmielecki J, Lin YL, et al. Lung cancers with acquired resistance to EGFR inhibitors occasionally harbor BRAF gene mutations but lack mutations in KRAS, NRAS, or MEK1. *Proceedings of the National Academy of Sciences of the United States of America*. 2012;109(31):E2127-33. PMID: 3411967.
58. Ramos P, Bentires-Alj M. Mechanism-based cancer therapy: resistance to therapy, therapy for resistance. *Oncogene*. 2015;34(28):3617-26.
59. Huang C, Park CC, Hilsenbeck SG, Ward R, Rimawi MF, Wang YC, et al. beta1 integrin mediates an alternative survival pathway in breast cancer cells resistant to lapatinib. *Breast cancer research : BCR*. 2011;13(4):R84. PMID: 3236347.

60. Politi K, Zakowski MF, Fan PD, Schonfeld EA, Pao W, Varmus HE. Lung adenocarcinomas induced in mice by mutant EGF receptors found in human lung cancers respond to a tyrosine kinase inhibitor or to down-regulation of the receptors. *Genes & development*. 2006;20(11):1496-510. PMID: 1475762.
61. Zheng H, Kang Y. Multilayer control of the EMT master regulators. *Oncogene*. 2014;33(14):1755-63.
62. Burns TF, Dobromilskaya I, Murphy SC, Gajula RP, Thiyagarajan S, Chatley SN, et al. Inhibition of TWIST1 leads to activation of oncogene-induced senescence in oncogene-driven non-small cell lung cancer. *Molecular cancer research : MCR*. 2013;11(4):329-38. PMID: 3631276.
63. Qin Q, Xu Y, He T, Qin C, Xu J. Normal and disease-related biological functions of Twist1 and underlying molecular mechanisms. *Cell research*. 2012;22(1):90-106. PMID: 3351934.
64. Niederst MJ, Engelman JA. Bypass mechanisms of resistance to receptor tyrosine kinase inhibition in lung cancer. *Science signaling*. 2013;6(294):re6. PMID: 3876281.
65. Girotti MR, Pedersen M, Sanchez-Laorden B, Viros A, Turajlic S, Niculescu-Duvaz D, et al. Inhibiting EGF receptor or SRC family kinase signaling overcomes BRAF inhibitor resistance in melanoma. *Cancer discovery*. 2013;3(2):158-67.
66. Wilson C, Nicholes K, Bustos D, Lin E, Song Q, Stephan JP, et al. Overcoming EMT-associated resistance to anti-cancer drugs via Src/FAK pathway inhibition. *Oncotarget*. 2014;5(17):7328-41. PMID: 4202126.
67. Eckert MA, Lwin TM, Chang AT, Kim J, Danis E, Ohno-Machado L, et al. Twist1-induced invadopodia formation promotes tumor metastasis. *Cancer cell*. 2011;19(3):372-86. PMID: 3072410.
68. Whitehead J, Vignjevic D, Futterer C, Beaurepaire E, Robine S, Farge E. Mechanical factors activate beta-catenin-dependent oncogene expression in APC mouse colon. *HFSP journal*. 2008;2(5):286-94. PMID: 2639941.
69. Rolfo C, Giovannetti E, Hong DS, Bivona T, Raez LE, Bronte G, et al. Novel therapeutic strategies for patients with NSCLC that do not respond to treatment with EGFR inhibitors. *Cancer treatment reviews*. 2014;40(8):990-1004.
70. Regales L, Gong Y, Shen R, de Stanchina E, Vivanco I, Goel A, et al. Dual targeting of EGFR can overcome a major drug resistance mutation in mouse models of EGFR mutant lung cancer. *The Journal of clinical investigation*. 2009;119(10):3000-10. PMID: 2752070.
71. Crystal AS, Shaw AT, Sequist LV, Fribolet L, Niederst MJ, Lockerman EL, et al. Patient-derived models of acquired resistance can identify effective drug combinations for cancer. *Science*. 2014;346(6216):1480-6. PMID: 4388482.

72. Tricker EM, Xu C, Uddin S, Capelletti M, Ercan D, Ogino A, et al. Combined EGFR/MEK Inhibition Prevents the Emergence of Resistance in EGFR-Mutant Lung Cancer. *Cancer discovery*. 2015;5(9):960-71.
73. Costa DB, Halmos B, Kumar A, Schumer ST, Huberman MS, Boggon TJ, et al. BIM mediates EGFR tyrosine kinase inhibitor-induced apoptosis in lung cancers with oncogenic EGFR mutations. *PLoS Med*. 2007;4(10):1669-79; discussion 80. PMID: 2043012.
74. Johnson ML, Riely GJ, Rizvi NA, Azzoli CG, Kris MG, Sima CS, et al. Phase II trial of dasatinib for patients with acquired resistance to treatment with the epidermal growth factor receptor tyrosine kinase inhibitors erlotinib or gefitinib. *Journal of thoracic oncology : official publication of the International Association for the Study of Lung Cancer*. 2011;6(6):1128-31. PMID: 3230574.
75. Mok TS. Personalized medicine in lung cancer: what we need to know. *Nature reviews Clinical oncology*. 2011;8(11):661-8.
76. Riely GJ, Marks J, Pao W. KRAS mutations in non-small cell lung cancer. *Proceedings of the American Thoracic Society*. 2009;6(2):201-5.
77. Stephen AG, Esposito D, Bagni RK, McCormick F. Dragging ras back in the ring. *Cancer cell*. 2014;25(3):272-81.
78. Collado M, Serrano M. Senescence in tumours: evidence from mice and humans. *Nature reviews Cancer*. 2010;10(1):51-7. PMID: 3672965.
79. Collado M, Gil J, Efeyan A, Guerra C, Schuhmacher AJ, Barradas M, et al. Tumour biology: senescence in premalignant tumours. *Nature*. 2005;436(7051):642.
80. Prieur A, Peeper DS. Cellular senescence in vivo: a barrier to tumorigenesis. *Current opinion in cell biology*. 2008;20(2):150-5.
81. Serrano M, Lin AW, McCurrach ME, Beach D, Lowe SW. Oncogenic ras provokes premature cell senescence associated with accumulation of p53 and p16INK4a. *Cell*. 1997;88(5):593-602.
82. Fernald K, Kurokawa M. Evading apoptosis in cancer. *Trends in cell biology*. 2013;23(12):620-33. PMID: 4091735.
83. Barnes RM, Firulli AB. A twist of insight - the role of Twist-family bHLH factors in development. *The International journal of developmental biology*. 2009;53(7):909-24. PMID: 2737731.
84. Pham CG, Bubici C, Zazzeroni F, Knabb JR, Papa S, Kuntzen C, et al. Upregulation of Twist-1 by NF-kappaB blocks cytotoxicity induced by chemotherapeutic drugs. *Molecular and cellular biology*. 2007;27(11):3920-35. PMID: 1900008.
85. Zhuo WL, Wang Y, Zhuo XL, Zhang YS, Chen ZT. Short interfering RNA

directed against TWIST, a novel zinc finger transcription factor, increases A549 cell sensitivity to cisplatin via MAPK/mitochondrial pathway. *Biochemical and biophysical research communications*. 2008;369(4):1098-102.

86. Cheng GZ, Chan J, Wang Q, Zhang W, Sun CD, Wang LH. Twist transcriptionally up-regulates AKT2 in breast cancer cells leading to increased migration, invasion, and resistance to paclitaxel. *Cancer research*. 2007;67(5):1979-87.

87. Ansieau S, Bastid J, Doreau A, Morel AP, Bouchet BP, Thomas C, et al. Induction of EMT by twist proteins as a collateral effect of tumor-promoting inactivation of premature senescence. *Cancer cell*. 2008;14(1):79-89.

88. Yang MH, Wu MZ, Chiou SH, Chen PM, Chang SY, Liu CJ, et al. Direct regulation of TWIST by HIF-1alpha promotes metastasis. *Nature cell biology*. 2008;10(3):295-305.

89. Cheng GZ, Zhang WZ, Sun M, Wang Q, Coppola D, Mansour M, et al. Twist is transcriptionally induced by activation of STAT3 and mediates STAT3 oncogenic function. *The Journal of biological chemistry*. 2008;283(21):14665-73. PMID: 2386910.

90. Karamouzis MV, Konstantinopoulos PA, Papavassiliou AG. Targeting MET as a strategy to overcome crosstalk-related resistance to EGFR inhibitors. *The Lancet Oncology*. 2009;10(7):709-17.

91. Franco HL, Casasnovas J, Rodriguez-Medina JR, Cadilla CL. Redundant or separate entities?--roles of Twist1 and Twist2 as molecular switches during gene transcription. *Nucleic acids research*. 2011;39(4):1177-86. PMID: 3045590.

92. Tsai CC, Chen YJ, Yew TL, Chen LL, Wang JY, Chiu CH, et al. Hypoxia inhibits senescence and maintains mesenchymal stem cell properties through down-regulation of E2A-p21 by HIF-TWIST. *Blood*. 2011;117(2):459-69.

93. Patel D, Chaudhary J. Increased expression of bHLH transcription factor E2A (TCF3) in prostate cancer promotes proliferation and confers resistance to doxorubicin induced apoptosis. *Biochemical and biophysical research communications*. 2012;422(1):146-51. PMID: 3361642.

94. Slyper M, Shahar A, Bar-Ziv A, Granit RZ, Hamburger T, Maly B, et al. Control of breast cancer growth and initiation by the stem cell-associated transcription factor TCF3. *Cancer research*. 2012;72(21):5613-24.

95. Chang AT, Liu Y, Ayyanathan K, Benner C, Jiang Y, Prokop JW, et al. An evolutionarily conserved DNA architecture determines target specificity of the TWIST family bHLH transcription factors. *Genes & development*. 2015;29(6):603-16. PMID: 4378193.

96. Hayashi M, Nimura K, Kashiwagi K, Harada T, Takaoka K, Kato H, et al. Comparative roles of Twist-1 and Id1 in transcriptional regulation by BMP signaling. *Journal of cell science*. 2007;120(Pt 8):1350-7.

97. Lamb J, Crawford ED, Peck D, Modell JW, Blat IC, Wrobel MJ, et al. The Connectivity Map: using gene-expression signatures to connect small molecules, genes, and disease. *Science*. 2006;313(5795):1929-35.
98. Fontaine F, Overman J, Francois M. Pharmacological manipulation of transcription factor protein-protein interactions: opportunities and obstacles. *Cell regeneration*. 2015;4(1):2. PMID: 4365538.



## Curriculum vitae

### JESSICA CADES

604 Hyson St., Baltimore, MD 21230 | 610-608-2633 | Jessica.cades@gmail.com

#### EDUCATION

Johns Hopkins University, Baltimore, MD

**Ph.D. in Pharmacology and Molecular Sciences**

**expected December 2015**

Drexel University, Philadelphia, PA

**B.S. in Chemical Engineering**

**June 2011**

ABET accredited program

Magna Cum Laude

#### AWARDS

AJ Drexel Academic Scholarship, *Drexel University*

**September 2006 – June 2011**

Dean's List, *Drexel University*

**September 2006 – June 2011**

National Merit Finalist

**2006**

#### EXPERIENCE

Johns Hopkins University, Baltimore, MD

**Graduate Student**

**August 2011 – current**

- Thesis project focusing on and exploring acquired resistance to erlotinib in EGFR mutant non-small cell lung cancer (NSCLC), particularly that of epithelial-mesenchymal transition (EMT) mediated by the transcription factor, Twist1
- Planned and carried out a variety of experiments involving the use and manipulation of cells
- Created and manipulated overexpression and knockdown lines through virus transfection in human cancer cell lines
- Handled transgenic mice
- Delivered drugs to mice by oral gavage and intraperitoneal (IP) injection
- Planned and carried out experiments utilizing transgenic mice
- Performed scientific literature searches for the purposes of researching methods, planning experiments, writing and reviewing abstracts and papers for publication
- Oversaw timely completion of own projects and others' work to ensure adherence to deadlines
- Prepared and delivered numerous presentations, both powerpoints and posters, to share research findings and recommendations with superiors, peers and other members of the scientific community as well as the general public
- Evaluated data and performed research to determine validity of scientific claims

- Participated in the formulation, writing and review of several professional publications

GlaxoSmithKline, Upper Merion, PA

**DMPK Bioanalytical Technology Exploration** **March – September 2010**

- Utilized dried blood spots (DBS) for quantification of small molecules and some large molecules (biopharmaceuticals)
- Reviewed, developed and evaluated methods for DBS for compounds
- Dealt with formulation issues that impacted drug product performance
- Prepared reports and presentations on scientific findings for management and other scientists
- Participated in discussions with other scientists and management to resolve problems and share information
- Operated ultra-high performance liquid chromatography (UPLC) and mass spectrometer in conjunction with DBS methods
- Worked with automatic liquid handlers, centrifuges and other lab equipment
- Performed extensive hand and automatic pipetting
- Made up standard curves and quality control samples in blood and plasma
- Carried out experiments looking at compound stability in dried blood spots for a poster, Feasibility of Dried Blood Spot Application to Stability of Glucuronides, and publication, Evaluation of glucuronide metabolite stability in dried blood spots, in the journal Bioanalysis

Aprexia Pharmaceuticals, Langhorne, PA

**Formulation Scientist** **March – September 2009**

- Formulated liquid binder for three-dimensional printing
- Provided expert technical advice on chemical engineering related to formulation development and drug product performance
- Tested properties of suspensions/fluids
- Operated Dyno-Mill for reduction of particle size
- Documented experiments in notebook
- Prepared reports and presentations on scientific findings for other scientists and management
- Received education on regulatory issues associated with pharmaceutical product manufacturing
- Received foundation Good Manufacturing Practices (GMP) Training

Merck, West Point, PA

**Assistant Engineer** **March – September 2008**

- Worked in Engineering Maintenance and Utilities for Biologics Pilot Plant
- Gained exposure to technical aspects of manufacturing of biologics and pharmaceutical product regulations

- Updated Piping and Instrumentation Drawings for cold rooms and clean steam distribution
- Ordered and researched spare parts for air compressors and valves
- Served as point of contact for vendors regarding preventative maintenance and quotes for parts
- Supervised painters and carpenters during building shutdown to assure timely completion of projects

## PUBLICATIONS

*Structure-function studies of the bHLH phosphorylation domain of Twist1 in prostate cancer cells.* Gajula RP, Chettiar ST, Williams RD, Nugent K, Kato Y, Wang H, Malek R, Taparra K, Cades J, Annadanam A, Yoon A, Fertig E, Firulli BA, Mazzacurati L, Burns TF, Firulli AB, An S, Tran PT. **Neoplasia** (2014). In press.

*An H3K36me3 binding PWWP protein targets the NuA3 acetyltransferase complex to coordinate transcriptional elongation at coding regions.* Gilbert TM, McDaniel SL, Byrum SD, Cades JA, Dancy BC, Wade H, Tackett AJ, Strahl BD, Taverna SD. **Mol Cell Proteomics**. 2014 Nov;13(11):2883-95. doi: 10.1074/mcp.M114.038224. Epub 2014 Aug 6.

*The twist box domain is required for Twist1-induced prostate cancer metastasis.* Gajula RP, Chettiar ST, Williams RD, Thiyagarajan S, Kato Y, Aziz K, Wang R, Gandhi N, Wild AT, Vesuna F, Ma J, Salih T, Cades J, Fertig E, Biswal S, Burns TF, Chung CH, Rudin CM, Herman JM, Hales RK, Raman V, An SS, Tran PT. **Mol Cancer Res**. 2013 Nov;11(11):1387-400. doi: 10.1158/1541-7786.MCR-13-0218-T. Epub 2013 Aug 27. PMID: 23982216

*Concurrent versus sequential sorafenib therapy in combination with radiation for hepatocellular carcinoma.* Wild AT, Gandhi N, Chettiar ST, Aziz K, Gajula RP, Williams RD, Kumar R, Taparra K, Zeng J, Cades JA, Velarde E, Menon S, Geschwind JF, Cosgrove D, Pawlik TM, Maitra A, Wong J, Hales RK, Torbenson MS, Herman JM, Tran PT. **PLoS One**. 2013 Jun 6;8(6):e65726. doi: 10.1371/journal.pone.0065726. Print 2013. PMID: 23762417

*Novel Hsp90 inhibitor NVP-AUY922 radiosensitizes prostate cancer cells.* Gandhi N, Wild AT, Chettiar ST, Aziz K, Kato Y, Gajula RP, Williams RD, Cades JA, Annadanam A, Song D, Zhang Y, Hales RK, Herman JM, Armour E, DeWeese TL, Schaeffer EM, Tran PT. **Cancer Biol Ther**. 2013 Apr;14(4):347-56. doi: 10.4161/cbt.23626. Epub 2013 Jan 28. PMID: 23358469

*Evaluation of glucuronide metabolite stability in dried blood spots.* Bowen CL, Volpatti J, Cades J, Licea-Perez H, Evans CA. **Bioanalysis**. 2012 Dec;4(23):2823-32. doi: 10.4155/bio.12.269. PMID: 23216122

#### MEMBERSHIPS

American Association for Cancer Research  
American Association for the Advancement of Science  
Tau Beta Pi Engineering Honor Society  
Phi Sigma Pi